Journal of Dermatological Science (2006) 42, 111—119

ELSEVIER

Dermatological SCIENCE

www.intl.elsevierhealth.com/journals/jods

Bone morphogenetic protein-2 modulates Wnt and frizzled expression and enhances the canonical pathway of Wnt signaling in normal keratinocytes

Lujun Yang, Kenshi Yamasaki, Yuji Shirakata *, Xiuju Dai, Sho Tokumaru, Yoko Yahata, Mikiko Tohyama, Yasushi Hanakawa, Koji Sayama, Koji Hashimoto

Department of Dermatology, Ehime University School of Medicine, Shitsukawa, Toon, Ehime 791-0295, Japan

Received 21 July 2005; received in revised form 6 December 2005; accepted 19 December 2005

KEYWORDS
BMP-2;
Frizzled;
Keratinocyte;
TCF/LEF;
Wnt

Summary

Background: Bone morphogenetic protein-2 (BMP-2) and Wnt are involved in the normal development and tumorigenesis of several organs, and in the development of skin and skin appendages as a morphogen. However, the crosstalk between BMP-2 and the Wnt/β-catenin signaling pathway is not clear.
Objective: We examined BMP-2-dependent expression of Wnt and its receptor frizzled in normal human keratinocytes.
Methods: The mRNA expression of the Wnt and frizzled families was analyzed by reverse transcription-polymerase chain reaction (RT-PCR) or ribonuclease protection assay. β-Catenin expression was measured using RT-PCR and Western blotting. T-cell factor/lymphoid enhancing factor activity was analyzed using the luciferase reporter assay.
Results: We detected the expression of Wnt-2b/13, -4, -5a, -5b, -7a, -7b, and -10a, frizzled-1, -4, -5, -6, -8, -9, and -10, MFRP, and SFRP-1/SARP-2 in keratinocytes. BMP-2 increased Wnt-2b/13, -5b, and -7b, and frizzled-6, -8, and -10. Conversely, BMP-2 suppressed Wnt-10a and SFRP-1/SARP-2. Although Wnt-4 expression was not affected by BMP-2 in confluent conditioned keratinocytes, BMP-2 suppressed cell density-dependent Wnt-4 induction. The transcriptional activity of TCF/LEF, which is a target of the canonical Wnt pathway, was upregulated by BMP-2 in both time- and dose-

Abbreviations: BHE, bovine hypothalamic extract; BMP, bone morphogenetic protein; GAPDH, glyceraldehyde-3-phosphate dehydrogenase; GSK-3β, glycogen synthase kinase-3; MFRP, membrane-type frizzled-related protein; SARP, secreted apoptosis-related protein; SFRP, secreted frizzled-related protein; TCF/LEF, T-cell factor/lymphoid enhancing factor

* Corresponding author. Tel.: +81 89 960 5350; fax: +81 89 960 5352.
E-mail address: shirakat@m.ehime-u.ac.jp (Y. Shirakata).

doi:10.1016/j.jdermsci.2005.12.011

dependent manners. However, BMP-2-dependent differentiation of keratinocytes suppressed TCF/LEF transcriptional activity.
Conclusion: These results suggest that BMP-2 modulates the expression of molecules involved in Wnt signaling, and activates the canonical Wnt pathway in normal human keratinocytes. Moreover, Wnt signaling may be influenced by the fate of keratinocytes, such as proliferation, migration, and differentiation.

1. Introduction

The Wnt family is a major gene family that is expressed in developing organs. Wnt genes encode secreted glycoproteins, and Wnt signals are involved in embryonic development, the generation of cell polarity, and the specification of cell fate [1]. Nineteen Wnt genes have been identified in humans [2], and at least four Wnt signaling pathways have been elucidated: the β-catenin pathway (canonical Wnt pathway), which activates target genes in the nucleus; the planar cell polarity pathway, which involves JNK (jun N-terminal kinase) and cytoskeletal rearrangements; the Wnt/Ca^{2+} pathway, which involves activation of PLC and PKC; and the pathway that regulates spindle orientation and asymmetric cell division [3]. Of these, the β-catenin pathway is essential for Wnt function, and has been studied intensely.

In the canonical pathway of Wnt signaling, Wnt transmits signals by binding to frizzled cell-surface receptors. Ten frizzled members have been identified in humans. Frizzled has seven transmembrane domains, a short cytoplasmic tail containing a consensus PSD-95/Dlg/ZO-1 homology (PDZ) domain-binding motif at the carboxyl terminus, and an amino-terminal cysteine-rich domain that binds Wnt [2]. Frizzled activates Disheveled, which inactivates glycogen synthase kinase-3β (GSK-3β), and saves β-catenin from ubiquitination and degradation [4]. Stabilized β-catenin accumulates in the cytoplasm and translocates to the nucleus, where it binds transcription factors of the T-cell factor/lymphoid enhancing factor (TCF/LEF) family, and activates the transcription of target genes, such as c-myc, cyclin D1, and c-jun, which are involved in carcinogenesis [3,5]. The Wnt/β-catenin signaling pathway has important roles in tumorigenesis and in the differentiation and patterning of diverse tissues during animal development [2]. Moreover, roles in the development of skin, hair, and related appendages have been suggested. For example, Wnt-3a and -7a can act as inductive signals to maintain dermal papillae in an anagen state [6]. Wnt-4 proteins are thought to be involved in epidermal–dermal interactions in mammalian skin [7]. The expression of mouse frizzled-3 is reported to be restricted to the epidermis and developing hair follicles, and a role in follicle development has been suggested [8].

Despite many studies of Wnt expression and its roles in animal skin, the factors and mechanisms that regulate the Wnt/β-catenin signaling pathway in skin are poorly understood. In epithelial–mesenchymal interactions in the initial morphogenesis of the mammalian tooth, both BMP and Wnt signaling activate Lef1 [9]. In cultured murine multipotent mesenchymal cell line C3H10T1/2, BMP-2 upregulates Wnt-3a expression and downregulates Wnt-7a expression [10]. BMP-2 is involved in tissue and organ development and in regulating epidermal induction and keratinocyte differentiation [11]. These data suggest that there is crosstalk between the BMP-2 and Wnt/β-catenin signals in human keratinocytes. In this report, we show that BMP-2 modulates the expression of the Wnt and frizzled families, and enhances the canonical pathway of Wnt signaling in normal human keratinocytes.

2. Materials and methods

2.1. Cell culture

Normal human keratinocytes from an excised polydactyl finger of 1-year-old boy were cultured in MCDB153 medium supplemented with insulin (5 $\mu g\ mL^{-1}$), hydrocortisone (5×10^{-7} M), ethanolamine (0.1 mM), phosphoethanolamine (0.1 mM), bovine hypothalamic extract (BHE) (50 $\mu g\ mL^{-1}$), and Ca^{2+} (0.1 mM), as described previously [12,13]. Third- to fifth-passage cells were used in all of the experiments. All procedures that involved human subjects received prior approval from the Ethics Committee of Ehime University School of Medicine, Toon, Ehime, Japan, and all subjects provided written informed consent.

2.2. Reagents

Recombinant BMP-2 was a generous gift from Yamanouchi Pharmaceutical (Tokyo, Japan). Anti-β-cate-

nin antibody was purchased from New England Biolabs (Beverly, MA, USA). Conditioned medium of Wnt-3a-expressing mouse fibroblasts L cells (L cells) and neomycin-expressing L cells were kind gifts from S. Takada, Center for Molecular and Developmental Biology, Graduate School of Science, Kyoto University, Kyoto, Japan [14].

2.3. RT-PCR analysis

Total RNA from cultured human keratinocytes was prepared with Isogen (Nippon Gene, Toyama, Japan) and treated with 50 U mL^{-1} of DNase 1 (Clontech Laboratories, Palo Alto, CA, USA) at 37 °C for 30 min to remove any contaminating genomic DNA. Specific primers for human frizzled and Wnt cDNA were generated by selecting specific nucleotide sequences corresponding to the following oligonucleotides (Table 1). Reverse transcription-polymerase chain reaction (RT-PCR) was performed using RT-PCR High Plus™ (Toyobo, Osaka, Japan) according to the manufacturer's instructions. Briefly, 1 μg of total RNA was added to a 50-μL reaction mixture containing 10 μL of 5× reaction buffer, 6 μL of 2.5 mM dNTPs, 5 μL of 25 mM $Mn(OAc)_2$, 19 μL of RNase-free H_2O, 2 μL of 10 U μL^{-1} RNase inhibitor, 2 μL of 2.5 U μL^{-1} of rTth DNA polymerase, and 2 μL of 10 pmol μL^{-1} of each primer. cDNA was reverse transcribed from total RNA for 30 min at 60 °C, and heated to 94 °C for 2 min. Amplification was performed using a DNA thermal cycler (Astec, Fukuoka, Japan) for 25–38 cycles. The cycle profile consisted of 1 min at 94 °C for denaturation, and 1.5 min at 60 °C for annealing and primer extension. To evaluate the amplification, 5 μL of the reaction mixture was electrophoresed on a 2.0% agarose gel containing ethidium bromide. The PCR products were sequenced to confirm the amplification. We performed at least three independent studies and confirmed similar results. A representative experiment is shown in the figures.

2.4. Oligonucleotide probe preparation

PCR amplified human cDNAs were inserted into the *Eco*RI and *Hind*III sites of the pPMG vector (PharMingen, San Diego, USA). The inserted cDNAs corresponded to the oligonucleotides described above. These inserted cDNAs were confirmed by nucleotide sequencing. The pPMG vector, including GAPDH cDNA (PharMingen), was used as the internal standard. We used the hFrizzled RPA templates set (PharMingen) to detect frizzled-2 to -6 and SFRP-1 and -2.

2.5. Ribonuclease protection assay

Single-stranded antisense riboprobes were prepared by in vitro transcription of human cDNA fragments, using the RiboQuant® In Vitro Transcription kit (PharMingen) in the presence of [α-^{32}P] UTP. Samples of total RNA (10 μg each) were hybridized with ^{32}P-labeled riboprobe, and digested with RNase using the RiboQuant® RPA kit (PharMingen) according to the manufacturer's instructions. The hybridization products were separated on a gel and exposed to a film, as described previously [15]. We performed at least three independent studies and confirmed similar results. A representative experiment is shown in the figures.

2.6. Western blot analysis

For total cellular protein extraction, cells were harvested by scraping with extraction buffer con-

Table 1 sequence and accession number for primers

Primers for	Sequence	Accession number	Primers for	Sequence	Accession number
Frizzled-1	1247–1561	AF072872	Wnt-4	683–874	AF316543
Frizzled-4	1373–1651	AB032471	Wnt-5a	594–770	L20861
Frizzled-7	726–956	BC015915	Wnt-5b	76–232	AB060966
Frizzled-8	748–964	AB043703	Wnt-6	399–540	NM006522
Frizzled-9	1253–1444	U82169	Wnt-7a	595–722	U53476
Frizzled-10	1571–1746	AB027464	Wnt-7b	19–126	AF062766
SFRP (secreted frizzled-related protein)-4	775–929	E288952	Wnt-8a	107–427	AB057725
SFRP-5/secreted apoptosis-related (SARP)	686–825	AF117758	Wnt-8b	176–456	NM003393
Membrane-type frizzled-related protein (MFRP)	1008–1128	AB055505	Wnt-10a	317–574	AY009400
Wnt-1	325–650	NM005430	Wnt-10b/12	848–1081	NM003394
Wnt-2	373–665	X07876	Wnt-11	678–877	Y12692
Wnt-2b/13	1318–1487	Z71621	—	884–1032	NM003395
Wnt-3	385–636	NM0307	Wnt-14b/15	283–412	AB063483
Wnt-3a	10–231	XM047539	Wnt-16	661–773	AF152584

taining 150 mM NaCl, 1% Nonidet P-40, 0.5% deoxycholate, 0.1% SDS, 50 mM Tris–HCl pH 7.4, and protease inhibitors, and sonicated on ice. Equal amounts of protein (2.5 μg/lane) were separated by sodium dodecyl sulfate-polyacrylamide gel electrophoresis (SDS-PAGE), and transferred to polyvinylidene difluoride membranes. The first antibodies were incubated overnight at 4 °C. The analysis was performed using the Vistra ECF kit (Amersham Biosciences K.K., Tokyo, Japan) and Fluoroimager (Molecular Dynamics, Sunnyvale, CA), as described previously [15]. We performed at least three independent studies and confirmed similar results. A representative experiment is shown in the figures.

2.7. Luciferase reporter assay

Keratinocytes were seeded at 4.0×10^4 cells per well in 12-well collagen-coated dishes (Iwaki Glass, Tokyo, Japan), and cultured in 1 mL of MCDB153 medium with BHE. The medium was replaced 48 h later with 1 mL of fresh MCDB153 without BHE, with 0.5 μg of TOPFLASH containing three copies of the TCF/LEF consensus sequence or FOPFLASH containing three copies of a mutated consensus sequence, and 10 ng of pRL-CMV (Promega, Madison, WI, USA) as an internal standard of transfection. The keratinocytes were transfected using FUGENE6™ (Roche Diagnostic, Tokyo, Japan) according to the manufacturer's instructions. After a 10-h transfection with the reporter gene, the medium was replaced with 1 mL of fresh MCDB153 without BHE, and various concentrations of BMP-2 or conditioned medium of Wnt-3a-expressing L cells were added (keratinocyes were subconfluent). The cells were harvested 72 h later (keratinocyes reached confluency), and luciferase activity was measured using the Dual-Luciferase Reporter Assay System (Promega) according to the manufacturer's instructions. The transfection efficiency was standardized using an internal control, pRL-CMV. The mean and standard deviation of the relative values obtained from three independent experiments were plotted on graphs. Statistical analysis was performed using Student's *t*-test.

3. Results

3.1. BMP-2 enhances Wnt and frizzled gene expression in normal human keratinocytes

To explore the effects of BMP-2 on the expression of Wnt and frizzled family members in human keratinocytes, we stimulated quiescent (confluent conditioned) normal human keratinocytes with BMP-2 and examined Wnt and frizzled mRNA expression. Expression of the 19 Wnt family members (Wnt-1, -2, -2b/13, -3, -3a, -4, -5a, -5b, -6, -7a, -7b, -8a, -8b, -10a, -10b, -11, -14, -14b/15, and -16) in normal

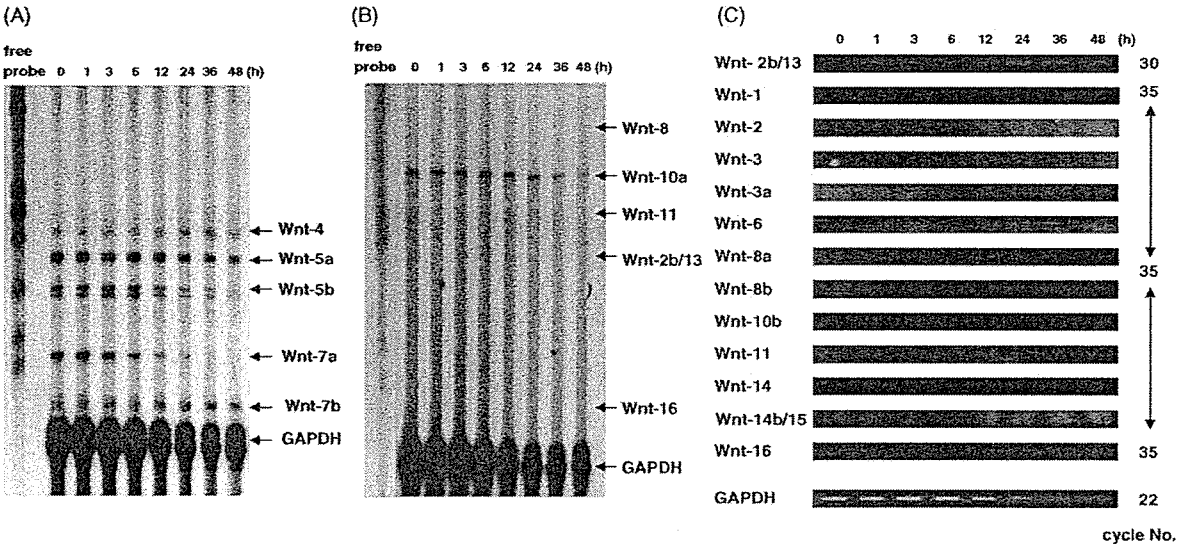

Fig. 1 BMP-2 modulates Wnt mRNA expression. (A and B) Keratinocytes were seeded and cultured until they reached subconfluence. After changing the medium to BHE-free MCDB153, the keratinocytes were cultured for a further 24 h. BMP-2 (4 ng mL^{-1}) was added to the keratinocyte culture medium, and total RNA was extracted 0, 1, 3, 6, 12, 24, 36, and 48 h after stimulation. Total RNA was hybridized with RNA probes, and separated on a polyacrylamide gel. GAPDH is the control mRNA. Three independent experiments were performed, and a representative experiment is shown. (C) Keratinocytes were stimulated, and total RNA was extracted as described above. Total RNA was used for RT-PCR, with the primers indicated to the left of the panel, and the cycle numbers indicated to the right. GAPDH was the control mRNA.

human epidermal keratinocytes was examined using a ribonuclease protection assay and RT-PCR. Of the Wnt family, Wnt-2b/13, -4, -5a, -5b, -7a, -7b, and -10a mRNAs were detected, while the other Wnt mRNAs were not (Fig. 1A–C). The expression of Wnt-2b/13 mRNA was upregulated beginning 24 h post-BMP-2 stimulation, and increased in a time-dependent manner (Fig. 1C). BMP-2 did not influence the expression of Wnt-4, -5a, and -7b mRNA (Fig. 1A). Wnt-10a decreased beginning 36 h post-BMP-2 stimulation (Fig. 1B). Wnt-5b increased transiently from 1 to 6 h, and decreased after 12 h (Fig. 1A). Wnt-7a mRNA increased transiently at 1 h, returned to the basal level at 3 h, decreased after 12 h, and was hardly detected after 36 h (Fig. 1A).

Next, we examined the expression of frizzled and related genes (frizzled-1, -2, -3, -4, -4s, -5, -6, -7, -8, -9, and -10, SFRP-1/SARP-2, SFRP-2/SARP-1, SFRP-4, SFRP-5/SARP-3, MFRP, and smoothened) using a ribonuclease protection assay and RT-PCR. We detected frizzled-5, -6, and SFRP-1/SARP-2 mRNA with the ribonuclease protection assay (Fig. 2A), and frizzled-1, -4, -8, -9, and -10, and membrane-type frizzled-related protein (MFRP) mRNA by RT-PCR (Fig. 2B). Although BMP-2 did not change the expression of frizzled-1, -4, -5, and -9, or MFRP mRNA, it upregulated frizzled-6 and -8 mRNA expression. Frizzled-6 expression increased beginning 6 h post-BMP-2 in a time-dependent manner. Frizzled-8 expression increased transiently from 3 to 24 h, and returned to the basal level by 36 h post-BMP-2. Frizzled-10 expression increased transiently from 3 to 12 h, and returned to the basal level by 36 h post-BMP-2. Interestingly, expression of one of the Wnt signal inhibitors, SFRP-1/SARP-2, decreased beginning 24 h post-BMP-2 in a time-dependent manner (Fig. 2A).

A previous report showed that the Wnt-4 mRNA level increased as normal murine keratinocytes approached confluence [7]. Therefore, we examined Wnt mRNA expression in the subconfluent to confluent condition (Fig. 3). We cultured keratinocytes and stimulated them with BMP-2 or vehicle at a cell density of 50%, and collected total mRNA at the indicated times. The final cell density 48 h post-BMP-2 stimulation was nearly confluent. Wnt-4 expression was upregulated when human keratinocytes reached confluence, as previously reported. Interestingly, BMP-2 suppressed cell density-dependent Wnt-4 induction. The level of Wnt-5a gene expression increased with the confluence of cultured cells of human mammary epithelial cell line HB2 [16]. In contrast, Wnt-5a expression was not

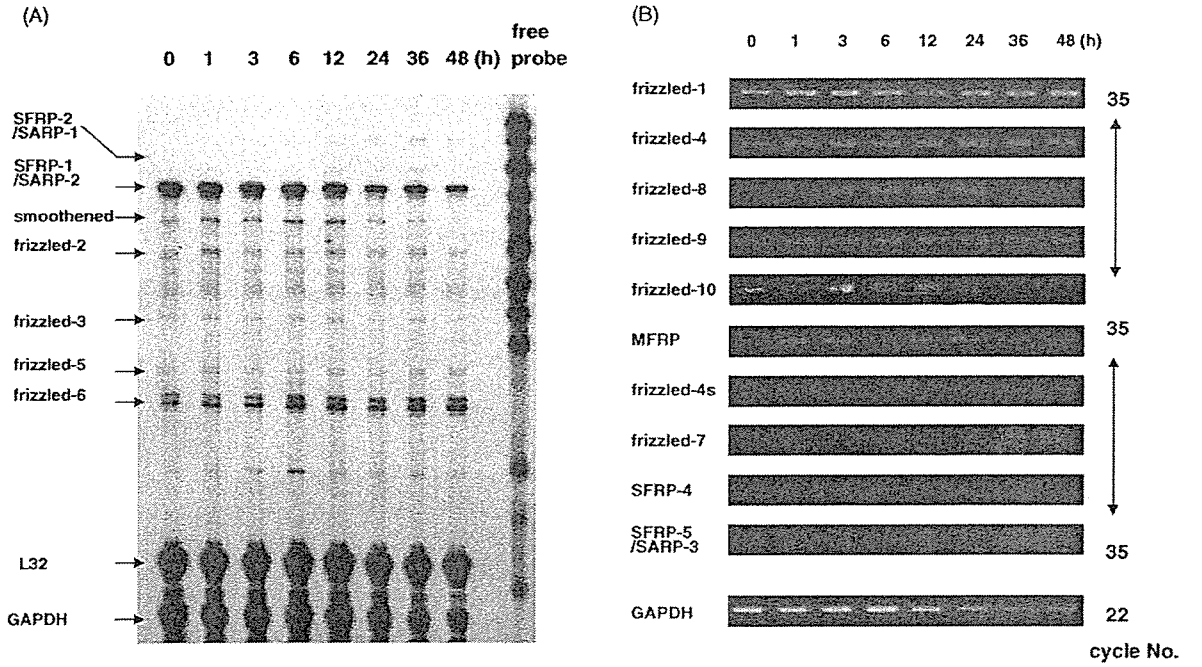

Fig. 2 BMP-2 modulates frizzled mRNA expression. (A) Keratinocytes were cultured and stimulated, and total RNA was extracted as described in the legend of Fig. 1A. Total RNA was hybridized with RNA probes, and separated on a polyacrylamide gel. L32 and GAPDH were the internal standards. (B) Keratinocytes were cultured and stimulated, and total RNA was extracted as described above and used for RT-PCR. The primers used are indicated to the left, and the cycle numbers to the right. GAPDH was the control mRNA.

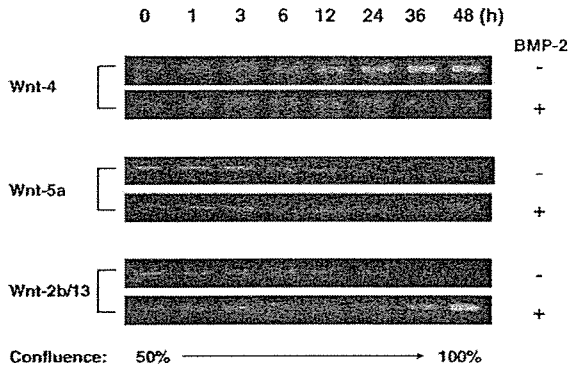

Fig. 3 BMP-2 increased Wnt-13 and decreased Wnt-4 mRNA expression. Keratinocytes were seeded and cultured until they reached 30–40% confluence. After changing the medium to BHE-free MCDB153, keratinocytes were cultured for a further 24 h. At this time, the keratinocytes reached about 50% confluence. BMP-2 (4 ng mL^{-1}) or vehicle was added to the keratinocyte culture medium, and total RNA was extracted 0, 1, 3, 6, 12, 24, 36, and 48 h after stimulation. The expression of Wnt-4, -5a, and -2b/13 was analyzed by RT-PCR.

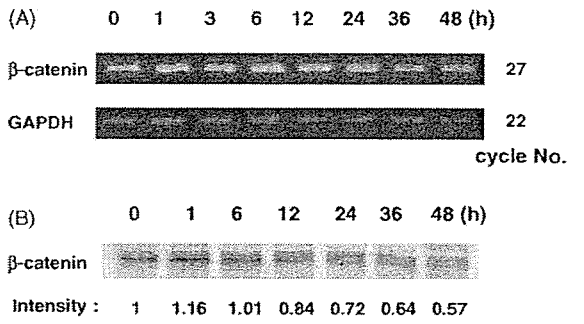

Fig. 4 BMP-2 did not enhance β-catenin expression. (A) BMP-2 (4 ng mL^{-1}) was added to the keratinocyte culture medium, and total RNA was extracted at indicated time points. The expression of β-catenin was analyzed by RT-PCR. (B) BMP-2 (4 ng mL^{-1}) was added to the keratinocyte culture medium, and cellular protein was extracted. Western blot analyses were performed with anti-β-catenin antibody. The intensity of each band was quantified, referring to the signal of the 0-h sample as 1 unit, and the mean of three independent studies is indicated.

enhanced with increasing cell density in human epidermal keratinocytes, and BMP-2 did not affect the cell density-dependent Wnt-5a expression pattern. Wnt-2b/13 decreased in a cell density-dependent manner, and BMP-2 increased Wnt-2b/13 expression in the confluent condition.

3.2. Effects of BMP-2 on β-catenin and TCF/LEF transcriptional activity

β-Catenin and TCF/LEF transcription factors are downstream targets of the Wnt canonical signaling pathway. Endogenous β-catenin activates TCF/LEF transcription activity [17]. We found that BMP-2 upregulated the expression of several Wnt and frizzled mRNAs. Therefore, we examined whether BMP-2 activates β-catenin for TCF/LEF signaling in human keratinocytes.

First, we examined the expression of β-catenin mRNA and protein in keratinocytes. BMP-2 did not change the expression of β-catenin mRNA (Fig. 4A). β-Catenin protein was transiently increased 1 h post-BMP-2 stimulation, returned to the basal level at 6 h, and then decreased in a time-dependent manner (Fig. 4B).

We then performed luciferase assays to examine TCF/LEF transcription activity. First, we examined TCF/LEF activity in keratinocytes using exogenous Wnt. We used conditioned medium of Wnt-3a-expressing L cells because Wnt-3a activates the canonical pathway [14]. Keratinocytes did not express Wnt-3a mRNA (Fig. 1C), so we did not need to consider the effect of intrinsic Wnt-3a. Keratinocytes were transfected with TOPFLASH, and then stimulated with Wnt-3a for 48 h. Wnt-3a increased the luciferase activity 6.3-fold compared with unstimulated keratinocytes, while control medium (conditioned medium of neomycin-expressing L cells) did not increase the luciferase activity (Fig. 5A). Next, we examined the effects of BMP-2 on TCF/LEF activity. Keratinocytes were transfected with TOPFLASH or FOPFLASH, and then stimulated with BMP-2 for 48 h. Luciferase activity was very low in FOPFLASH-transfected cells, and remained unchanged with BMP-2 (Fig. 5B). TOPFLASH activity in keratinocytes was significantly elevated with BMP-2 relative to the basal level. Upregulation occurred in both time- and dose-dependent manners (Fig. 5B and C). The presence of 2 ng mL^{-1} BMP-2 increased the TOPFLASH luciferase activity 2-fold, and 4 ng mL^{-1} increased it 3.5-fold relative to the basal level. However, 10 ng mL^{-1} BMP-2 only increased TOPFLASH luciferase activity 1.4-fold; because 10 ng mL^{-1} BMP-2 also induced striking morphological changes (stratification and enlargement) in cultured cells after a 48-h stimulation (unpublished data), the reduced luciferase activity is thought to result from keratinocyte differentiation. The combination of BMP-2 and Wnt-3a induced more transcription than did either BMP-2 or Wnt-3a alone (Fig. 5D). Therefore, BMP-2 enhanced TOPFLASH transcription synergistically with Wnt-3a, which suggests that BMP-2 modulates Wnt and frizzled expression, and enhances the canonical pathway of Wnt signaling.

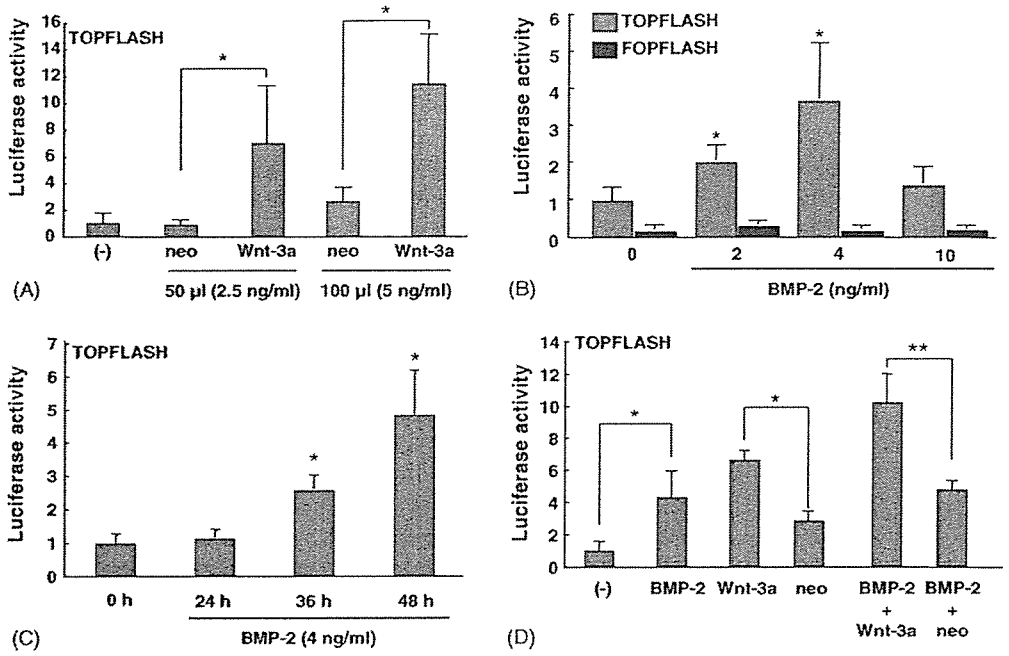

Fig. 5 BMP-2 enhances the canonical Wnt signal pathway. (A) Keratinocytes were seeded at 4.0×10^4 per well in 12-well collagen-coated dishes, and cultured in 1 mL of MCDB153 medium with BHE. After 48 h, the medium was replaced with 1 mL of fresh MCDB153 without BHE, and 0.5 μg of TOPFLASH and 10 ng of pRL-CMV were transfected. After a 10-h transfection of the reporter gene, the medium was replaced with 1 mL of fresh MCDB153 without BHE. Various concentrations of conditioned medium of L cells that expressed the Wnt-3a gene or neomycin (control vector) were added to the medium, and the cells were incubated for 72 h. Cells were harvested, and luciferase activity was measured. The luciferase activity of each sample was normalized against that of a non-stimulated sample. (B) Keratinocytes were cultured as described above, and transfected with 0.5 μg of TOPFLASH or FOPFLASH and 10 ng of pRL-CMV. After a 10-h transfection of the reporter gene, the medium was replaced with 1 mL of fresh MCDB153 without BHE. Various concentrations of BMP-2 were added to the medium and the cells were incubated for 72 h. The luciferase activity of each sample was normalized against that of a TOPFLASH-transfected, non-stimulated sample. (C) Keratinocytes were cultured as described above, and transfected with 0.5 μg of TOPFLASH and 10 ng of pRL-CMV. After a 10-h transfection of the reporter gene, the medium was replaced with 1 mL of fresh MCDB153 without BHE. BMP-2 (4 ng mL^{-1}) was added to the medium 24, 36, and 48 h before the cells were harvested, and luciferase activity was measured. The luciferase activity of each sample was normalized against that of a non-stimulated sample. (D) Keratinocytes were cultured as described above, and transfected with 0.5 μg of TOPFLASH and 10 ng of pRL-CMV. After a 10-h transfection of the reporter gene, the medium was replaced with 1 mL of fresh MCDB153 without BHE. BMP-2 (4 ng mL^{-1}) in combination with conditioned medium (5 ng mL^{-1}) of L cells that expressed the Wnt-3a gene or neomycin (control vector) were added to the medium, and the cells were incubated for 72 h. The luciferase activity of each sample was normalized against that of a non-stimulated sample. The bars and error bars represent the mean and S.D. of three independent experiments ($^{*}p < 0.05$ and $^{**}p < 0.01$).

4. Discussion

By definition, both BMP-2 and Wnts are morphogens that specify different cell fates in concentration-dependent manners [18]. BMP-2 could induce epidermal fate of ectodermal cells during embryogenesis, and regulate hair follicle development [19–21]. Several reports revealed the roles of Wnts, Frizzleds, and β-catenin in regulating skin and hair development which suggested Wnt/β-catenin pathway might be involved [22–24]. In our experiment, Wnt-2b/13, -4, -5a, -5b, -7a, -7b, and -10a mRNAs were detected in keratinocytes, and BMP-2 increased Wnt-2b/13, and decreased Wnt-10a. Wnt-5b and -7a increased transiently soon after BMP-2 stimulation, and later decreased (Fig. 1). Interestingly, although BMP-2 did not decrease Wnt-4 expression in the confluent condition, BMP-2 suppressed cell density-dependent Wnt-4 induction (Figs. 1 and 3). In contrast, BMP-2 increased Wnt-2b/13 in both the confluent and sub-confluent conditions (Figs. 1 and 3). These results suggest that BMP-2 modulates Wnt expression in keratinocytes, and cell confluence affects BMP-2-dependent Wnt induction. BMP-2 modulates the expression of Wnt-3a and -7a mRNA, and BMP-2 can upregulate the activity of lef1 in the murine

multipotent mesenchymal cell line C3H10T1/2 [9,10]. In hair budding, however, BMP induces E-cadherin by suppressing Lef1 activation, and the balance between the BMP and Wnt signals regulates proper hair budding [25]. Therefore, cell types and cell conditions, such as proliferation, differentiation, and the cell environment, may influence the interaction between BMP-2 and Wnt.

In the frizzled family, BMP-2 increased frizzled-6 in a time-dependent manner, and transiently increased frizzled-8 and -10 (Fig. 2). These results suggest that BMP-2-treated keratinocytes are susceptible to Wnt stimulation. Interestingly, human keratinocytes express abundant SFRP-1/SARP-2 mRNA, and BMP-2 suppressed SFRP-1/SARP-2 expression (Fig. 2). SFRP/SARP mRNAs encode secreted proteins that possess a cysteine-rich domain homologous to those of frizzled proteins, but lack the transmembrane regions that are characteristic of frizzled-like proteins. It has been suggested that SFRP/SARPs bind to Wnt and interfere with the interaction between Wnt and frizzled, resulting in Wnt signal suppression, because SFRP-1/SARP-2 decreases the intracellular β-catenin concentration in cultured human breast adenocarcinoma MCF7 cells [26]. The increases in frizzled-6, -8, and -10, and the decrease in SFRP-1/SARP-2 by BMP-2 suggest that frizzled-6, -8, and -10, and SFRP-1/SARP-2 enhance the Wnt signaling pathway with BMP-2 stimulation in a coordinated manner.

TCF/LEF members, originally cloned as lymphoid transcription factors, are recognized as potent transactivators on interaction with β-catenin, the downstream target of Wnt signaling [27]. BMP-2 upregulated the transcriptional activity of TCF/LEF in human keratinocytes, and BMP-2 enhanced Wnt-3a-dependent TCF/LEF activation (Fig. 5). BMP-2 upregulated the expression of some members, such as Wnt-2b/13 and frizzled-6, which suggests that these Wnt and frizzled genes are involved in the subsequent activation of TCF/LEF in human keratinocytes. Other mechanisms may also be involved in BMP-2-dependent TCF/LEF activation. The BMP-2 signal is transduced by the smad family, and smad4 interacts with TCF/LEFs directly [28]. Thus, smad4, which is activated by BMP-2 signaling and translocated into the nucleus, may activate TCF/LEF directly, and support Wnt-3a-dependent TCF/LEF activation. At the least, BMP-2 enhanced the canonical Wnt pathway in normal human keratinocytes under certain conditions. However, 10 ng mL^{-1} of BMP-2 did not activate the canonical Wnt pathway (Fig. 5B). This may be the effect of keratinocyte differentiation because 10 ng mL^{-1} of BMP-2 induced morphological changes in some genes that are induced in differentiated keratinocytes (unpublished data). Cell differentiation affects the expression of some Wnt, frizzled, and TCF/LEF genes [7,8,29]. Therefore, strong BMP-2 stimulation induces keratinocyte differentiation, and may not enhance TOPFLASH luciferase activity.

The particular stem cell lineage and stage of differentiation of the skin cell may influence the cell response to Wnt/β-catenin signaling. Mutated β-catenin without transcriptional activity acts in epidermis to promote hair fate and in hair cells to promote epidermal fate [30]; skin stem cells fail to differentiate into follicular KC in the absence of β-catenin, but instead adopt an epidermal fate [22]. In cultured normal human keratinocytes, we showed BMP-2 modulates the expression of molecules related to Wnt signaling and activates the canonical Wnt pathway, and Wnt signaling may be affected by the fate of keratinocytes, such as their proliferation, migration and differentiation. However, the target genes of TCF/LEF activated by BMP-2 in normal human keratinocytes are not clear. It is our future concern to reveal the target genes and the downstream biological/cellular events which might be influenced by these target genes in normal human keratinocytes.

In conclusion, BMP-2 modulates the expression of molecules related to Wnt signaling and activates the canonical Wnt pathway in normal human keratinocytes. Moreover, Wnt signaling may be affected by the fate of keratinocytes, such as their proliferation, migration, and differentiation.

Acknowledgments

This work was partly supported by Health Sciences Research Grants for Research on Specific Diseases from the Ministry of Health, Labor, and Welfare of Japan and a Grant-in-Aid for Scientific Research from the Ministry of Education, Culture, Sports, Science, and Technology of Japan. We thank Teruko Tsuda and Eriko Tan for technical assistance.

References

[1] Cadigan KM, Nusse R. Wnt signaling: a common theme in animal development. Genes Dev 1997;11:3286–305.
[2] Miller JR. The Wnts. Genome Biol 2002;3 [REVIEWS3001, Epub 2001 December 28].
[3] Huelsken J, Birchmeier W. New aspects of Wnt signaling pathways in higher vertebrates. Curr Opin Genet Dev 2001;11:547–53.
[4] van Gijn ME, Snel F, Cleutjens JP, Smits JF, Blankesteijn WM. Overexpression of components of the Frizzled–Dishevelled cascade results in apoptotic cell death, mediated by beta-catenin. Exp Cell Res 2001;265:46–53.

[5] Behrens J. Control of beta-catenin signaling in tumor development. Ann N Y Acad Sci 2000;910:21–33.
[6] Kishimoto J, Burgeson RE, Morgan BA. Wnt signaling maintains the hair-inducing activity of the dermal papilla. Genes Dev 2000;14:1181–5.
[7] Saitoh A, Hansen LA, Vogel JC, Udey MC. Characterization of Wnt gene expression in murine skin: possible involvement of epidermis-derived Wnt-4 in cutaneous epithelial–mesenchymal interactions. Exp Cell Res 1998;243:150–60.
[8] Hung BS, Wang XQ, Cam GR, Rothnagel JA. Characterization of mouse Frizzled-3 expression in hair follicle development and identification of the human homolog in keratinocytes. J Invest Dermatol 2001;116:940–6.
[9] Dassule HR, McMahon AP. Analysis of epithelial–mesenchymal interactions in the initial morphogenesis of the mammalian tooth. Dev Biol 1998;202:215–27.
[10] Fischer L, Boland G, Tuan RS. Wnt signaling during BMP-2 stimulation of mesenchymal chondrogenesis. J Cell Biochem 2002;84:816–31.
[11] Suzuki A, Kaneko E, Ueno N, Hemmati-Brivanlou A. Regulation of epidermal induction by BMP2 and BMP7 signaling. Dev Biol 1997;189:112–22.
[12] Shirakata Y, Tokumaru S, Yamasaki K, Sayama K, Hashimoto K. So-called biological dressing effects of cultured epidermal sheets are mediated by the production of EGF family, TGF-beta and VEGF. J Dermatol Sci 2003;32:209–15.
[13] Shirakata Y, Ueno H, Hanakawa Y, Kameda K, Yamasaki K, Tokumaru S, et al. TGF-beta is not involved in early phase growth inhibition of keratinocytes by 1alpha,25(OH)2Vitamin D3. J Dermatol Sci 2004;36:41–50.
[14] Shibamoto S, Higano K, Takada R, Ito F, Takeichi M, Takada S. Cytoskeletal reorganization by soluble Wnt-3a protein signalling. Genes Cells 1998;3:659–70.
[15] Yamasaki K, Hanakawa Y, Tokumaru S, Shirakata Y, Sayama K, Hanada T, et al. Suppressor of cytokine signaling 1/JAB and suppressor of cytokine signaling 3/cytokine-inducible SH2 containing protein 3 negatively regulate the signal transducers and activators of transcription signaling pathway in normal human epidermal keratinocytes. J Invest Dermatol 2003;120:571–80.
[16] Huguet EL, Smith K, Bicknell R, Harris AL. Regulation of Wnt5a mRNAexpression in human mammary epithelial cells by cell shape, confluence, and hepatocyte growth factor. J Biol Chem 1995;270:12851–6.
[17] Zhu AJ, Watt FM. Beta-catenin signalling modulates proliferative potential of human epidermal keratinocytes independently of intercellular adhesion. Development 1999;126:2285–98.
[18] Christian JL. BMP, Wnt and Hedgehog signals: how far can they go? Curr Opin Cell Biol 2000;12:244–9.
[19] Botchkarev VA, Botchkareva NV, Sharov AA, Funa K, Huber O, Gilchrest BA. Modulation of BMP signaling by noggin is required for induction of the secondary (nontylotrich) hair follicles. J Invest Dermatol 2002;118:3–10.
[20] Qiao W, Li AG, Owens P, Xu X, Wang XJ, Deng CX. Hair follicle defects and squamous cell carcinoma formation in Smad4 conditional knockout mouse skin. Oncogene 2005.
[21] Suzuki A, Kaneko E, Ueno N, Hemmati-Brivanlou A. Regulation of epidermal induction by BMP2 and BMP7 signaling. Dev Biol 1997;189:112–22.
[22] Huelsken J, Vogel R, Erdmann B, Cotsarelis G, Birchmeier W. Beta-catenin controls hair follicle morphogenesis and stem cell differentiation in the skin. Cell 2001;105:533–45.
[23] Reddy S, Andl T, Bagasra A, Lu MM, Epstein DJ, Morrisey EE, et al. Characterization of Wnt gene expression in developing and postnatal hair follicles and identification of Wnt5a as a target of Sonic hedgehog in hair follicle morphogenesis. Mech Dev 2001;107:69–82.
[24] Reddy ST, Andl T, Lu MM, Morrisey EE, Millar SE. Expression of Frizzled genes in developing and postnatal hair follicles. J Invest Dermatol 2004;123:275–82.
[25] Jamora C, DasGupta R, Kocieniewski P, Fuchs E. Links between signal transduction, transcription and adhesion in epithelial bud development. Nature 2003;422:317–22.
[26] Melkonyan HS, Chang WC, Shapiro JP, Mahadevappa M, Fitzpatrick PA, Kiefer MC, et al. SARPs: a family of secreted apoptosis-related proteins. Proc Natl Acad Sci USA 1997;94:13636–41.
[27] Roose J, Clevers H. TCF transcription factors: molecular switches in carcinogenesis. Biochim Biophys Acta 1999;1424:M23–37.
[28] Pukrop T, Gradl D, Henningfeld KA, Knochel W, Wedlich D, Kuhl M. Identification of two regulatory elements within the high mobility group box transcription factor XTCF-4. J Biol Chem 2001;276:8968–78.
[29] Zhou P, Byrne C, Jacobs J, Fuchs E. Lymphoid enhancer factor 1 directs hair follicle patterning and epithelial cell fate. Genes Dev 1995;9:700–13.
[30] DasGupta R, Rhee H, Fuchs E. A developmental conundrum: a stabilized form of beta-catenin lacking the transcriptional activation domain triggers features of hair cell fate in epidermal cells and epidermal cell fate in hair follicle cells. J Cell Biol 2002;158:331–44.

STEM CELLS
TISSUE-SPECIFIC STEM CELLS

Identification of Human Oral Keratinocyte Stem/Progenitor Cells by Neurotrophin Receptor p75 and the Role of Neurotrophin/p75 Signaling

TAKAHIRO NAKAMURA,[a,b] KEN-ICHI ENDO,[a] SHIGERU KINOSHITA[a]

[a]Department of Ophthalmology, Kyoto Prefectural University of Medicine, Graduate School of Medicine, Kyoto, Japan; [b]Research Center for Regenerative Medicine, Doshisha University, Kyoto, Japan

Key Words. p75 • Oral mucosa • Keratinocyte • Stem cell • Clonal analysis • Neurotrophin

ABSTRACT

This study was undertaken to determine whether human oral keratinocyte stem cells characteristically express higher levels of the low-affinity neurotrophin receptor p75 and to elucidate the function of p75 in oral keratinocytes. Examination of their expression patterns and cell-cycling status in vivo showed that p75 was exclusively expressed in the basal cell layer of both the tips of the papillae and the deep rete ridges. These immunostaining patterns suggest a cluster organization; most p75(+) cells did not actively cycle in vivo. Cell sorting showed that cells in the p75(+) subset were smaller and possessed higher in vitro proliferative capacity and clonal growth potential than the p75(−) subset. Clonal analysis revealed that holoclone-type (stem cell compartment), meroclone-type (intermediate compartment), and paraclone-type (transient amplifying cell compartment) cells, previously identified in skin and the ocular surface, were present in human oral mucosal epithelium. Holoclone-type cells showed stronger p75 expression at both the mRNA and protein level than did meroclone- and paraclone-type cells. Among the several neurotrophins, nerve growth factor (NGF) and neurotrophin-3 stimulated p75(+) oral keratinocyte cell proliferation, and only NGF protected them from apoptosis. Our in vivo and in vitro findings indicate that p75 is a potential marker of oral keratinocyte stem/progenitor cells and that some neurotrophin/p75 signaling affects cell growth and survival. STEM CELLS *2007;25:628–638*

INTRODUCTION

Epithelial cells, such as epidermal, esophageal, corneal, and oral keratinocytes, are organized into multiple layers. Like other rapidly renewing tissues, such as the hemopoietic system, the human epithelium is constantly regenerating. In general, proliferation occurs in the basal layer of keratinocytes attached to the underlying basement membrane; cells that undergo terminal differentiation as they migrate through the suprabasal layers are shed from the tissue surface [1]. Stem cells (SCs) facilitate the maintenance of self-renewing tissues; they are critical for replenishing and maintaining the cell balance (homeostasis) within tissues and for regenerating damaged tissue. Based on previous studies of several tissue types, criteria for keratinocyte SCs prescribe that they are relatively undifferentiated both ultrastructurally and biochemically; retain a high capacity for long-term, error-free self-renewal; have high proliferative potential; cycle slowly or rarely in vivo; are stimulated to proliferate in response to injury and certain growth stimuli; and are usually found in well-protected, highly vascularized and innervated areas [2–6]. It is generally known that SCs infrequently divide, yet they can proliferate soon in response to injury and certain growth stimuli, resulting in one SC and one transient amplifying cell (TAC) with limited proliferative potential. TACs are responsible for most routine proliferative activities; they are capable of extensive expansion of the cell population [7, 8]. Upon exhaustion of their proliferative potential, the rapidly proliferating TACs undergo terminal differentiation.

In this study, we used clonal analysis and cell sorting techniques for the purpose of characterizing the tissue SC and TAC populations. Clonal analysis identified three types of keratinocytes with different capacities for multiplication in human epidermis, hair follicles, and ocular surface epithelium [9–11]. Holoclones have the highest reproductive capacity, in paraclones, all cells undergo terminal differentiation within a few generations, and the behavior of meroclones is intermediate between holoclones and paraclones. Holoclones, meroclones, and paraclones are considered to be SCs, young TACs, and TACs, respectively. The holoclone-meroclone-paraclone transition is a unidirectional process that occurs during natural cell aging and during repeated subcultivation.

The cell-sorting technique uses phenotypic cell surface markers that distinguish differentiated cells from progenitor cells. Interesting results have been obtained in several tissue types. In human epidermis, SCs could be distinguished from differentiated keratinocytes by their higher expression of $\beta 1$ integrins [12, 13] and the combination of high levels of $\alpha 6$ integrin and low-to-undetectable levels of the transferring receptor (CD71) [14, 15]. For the further molecular characterization of various keratinocyte SCs, additional cell surface markers are needed.

The human oral cavity contains masticatory mucosa, such as gingiva, and lining mucosa, such as buccal mucosa. Oral mucosal epithelium has drawn attention as a cell source for a

Correspondence: Takahiro Nakamura, M.D., Ph.D., Department of Ophthalmology, Kyoto Prefectural University of Medicine, Kawaramachi Hirokoji, Kamigyo-ku, Kyoto 602-0841, Japan. Telephone: 81-75-251-5578; Fax: 81-75-251-5663; e-mail: tnakamur@ophth.kpu-m.ac.jp
Received August 7, 2006; accepted for publication November 9, 2006; first published online in STEM CELLS *EXPRESS* November 16, 2006.
 1066-5099/2007/$30.00/0 doi: 10.1634/stemcells.2006-0494

variety of tissue-engineered reconstructions, such as oral cavity [16], epidermis [17], and especially ocular surface reconstruction [18–23], and the transplantation of human oral epithelial sheets grown on various substrates can be useful for tissue reconstruction. In the clinical setting, the quality of the cultivated graft is the key to success, and the selection of a large number of highly proliferating oral epithelial cells, such as SCs and TACs, enhances the reproducibility, quality, and longevity of these grafts. However, little is known about oral keratinocyte SCs and TACs.

The p75 molecule, a low-affinity neurotrophin receptor, is a member of the tumor necrosis factor receptor superfamily [24]; its function is to mediate cell survival, apoptosis, and intercellular signaling in neuronal tissues [25, 26]. There is experimental evidence that p75 is also involved in controlling the fate of murine keratinocyte SCs through cell-cell interactions [27] and that it characterizes esophageal keratinocyte SCs in vitro [28]. However, its function in various human keratinocyte SCs remains to be fully elucidated.

We investigated the fate of p75(+) cells to determine whether this subset is critical for stem- or progenitor-cell lineages in human oral keratinocytes. Using clonal analysis and cell sorting, we evaluated the p75 expression patterns of human oral mucosal tissue and attempted to identify and isolate human oral keratinocyte stem/progenitor cells. We then investigated the effect of neurotrophin/p75 signaling in isolated oral keratinocytes. We found that human oral keratinocyte stem/progenitor cell phenotypes are characterized by their expression of p75 and that some neurtrophin/p75 signaling affected cell proliferation and survival.

MATERIALS AND METHODS

Tissues

Oral tissues were obtained from healthy volunteers and as superfluous tissue from patients undergoing oral surgery. We followed the tenets of the Declaration of Helsinki; all donors provided proper informed consent for biopsy. All samples were processed within 1–2 hours of harvest.

Cell Culture

For culture of the human oral epithelial cells, we used our previously reported system [18–20]. Briefly stated, submucosal connective tissues were removed with scissors to the extent possible; the resulting samples were cut into small explants. These were incubated (37°C, 1 hour) with 1.2 IU of Dispase (Roche, Indianapolis, http://www.roche.com) and treated with 0.05% trypsin-EDTA solution (10 minutes, room temperature) to separate the cells. The cell suspension was filtered through a cell dissociation sieve (Sigma-Aldrich, St. Louis, http://www.sigmaaldrich.com) to remove unsatisfactory segments; this yielded a suspension of purified oral epithelial cells. Isolated cell suspensions were then subjected to cell-sorting assay and clonal analysis.

Clonal Analysis

For clonal analysis, we applied the method of Barrandon and Green [9]. Secondary cultures of oral epithelial cells were used. Briefly stated, single cells, isolated under an inverted microscope, were inoculated into 12-well plates that contained a feeder layer of mitomycin C (MMC)-inactivated NIH-3T3 fibroblasts. After 7 days, a single clone was identified under an inverted microscope and photographed. Each clone was then divided into three parts; 5/8 of the clone was used for real-time polymerase chain reaction (PCR) assay, and 1/8 was subjected to immunocytochemical analysis to evaluate the cell characteristics. The other 1/4 of the clone was transferred to an indicator dish, fixed 10–12 days later, and stained with 0.1% toluidine blue for classification of the clonal type, which was determined by the percentage of aborted colonies [9]. When 0%–5% of the colonies were terminal, the clone was classified as a holoclone. When all colonies were terminal or when no colonies formed, the clone was classified as a paraclone, and when >5% but <100% of the colonies were terminal, the clone was classified as a meroclone.

Antibodies and Reagents

The following mouse monoclonal antibodies (mAbs) were used: anti-p75 (dilution, ×200) (Chemicon, Temecula, CA, http://www.chemicon.com; Abcam, Cambridge, U.K., http://www.abcam.com; and Upstate Biotech, Lake Placid, NY, http://www.upstate.com), anti-desmoplakin (×1) (Progen, Heidelberg, Germany, http://www.progen.de), anti-keratin 4 (×200)/10 (×50)/13 (×200) (Novocastra Ltd., Newcastle upon Tyne, U.K., http://www.novocastra.co.uk), anti-integrin α6 (×200)/β4 (×500)/α3 (×50)/β1 (×500) (Chemicon), CD34 (×50) (BD Biosciences, San Diego, http://www.bdbiosciences.com), CD71 (×50) (YLEM, Roma, Italy, http://www.ylem.it), BCRP (×10) (Kamiya Biomedical, Seattle, http://kamiyabiomedical.com/), and anti-Ki67 (×100) (Dako, Kyoto, Japan, http://www.dako.com). Rabbit polyclonal antibodies were also used: anti-ZO1 (×25) (Zymed, South San Francisco, CA, http://www.invitrogen.com) and anti-Ki67 (×50) (Abcam). Secondary antibodies were Alexa Fluor-488 goat anti-mouse or rabbit IgG (×1,500) and Alexa Fluor-594 goat anti-mouse or rabbit IgG (×1,500) (Molecular Probes Inc., Eugene, OR, http://probes.invitrogen.com). The following neurotrophins were used: nerve growth factor (NGF), brain-derived neurotrophic factor (BDNF), neurotrophin-3 (NT-3), and neurotrophin-4 (NT-4) (Sigma-Aldrich).

Cell Fractionation

The p75(+) and p75(−) cells were separated using magnetic cell sorting with the indirect microbead system (MACS; Miltenyi Biotec, Bergisch Gladbach, Germany, http://www.miltenyibiotec.com). The oral epithelial cell suspensions were labeled with anti-p75 mAb (×400) at 0°C for 15 minutes. The cells were then carefully washed with MACS buffer (phosphate-buffered saline [PBS] supplemented with 2 mM EDTA and 0.5% bovine serum albumin), incubated with rat anti-mouse IgG_1 microbeads (×5) at 4°C for 15 minutes, and exposed to the magnetic field of a permanent magnet on columns containing a ferromagnetic matrix. To increase the purity of the positive fraction, our protocol combined depletion columns and positive selection columns.

Validation of the Cell-Sorting Procedure

Flow Cytometry and Immunofluorescence. After the MACS procedure, each p75(+) and p75(−) cell fraction was again washed with MACS buffer and stained with Alexa Fluor-488 goat anti-mouse IgG (×1,500) at 4°C for 20 minutes for subsequent flow cytometric analysis (FACSCalibur; BD Biosciences) and immunofluorescence study. The cells were coverslipped using antifading mounting medium and examined under an immunofluorescence microscope (Olympus, Tokyo, http://www.olympus-global.com).

Reverse Transcription PCR. Total RNA was isolated from each isolated cell fraction using TRIzol reagent in accordance with the manufacturer's protocol. Complementary DNA was generated by mixing the extracted RNA (1 μg/μl per sample) with a random hexamer primer and AMV Reverse Transcriptase XL (Takara, Tokyo, http://www.takara.co.jp). The primers and PCR conditions were followed the previously reported method [28]. The expected product sizes were 230 base pairs (bp) for p75 and 541 bp for β-actin.

Measurement of Cell Area

Each isolated cell fraction was centrifuged and resuspended in culture medium. Cells (approximately 10^3 cells) in 10 ml of medium were placed in 100-mm culture dishes and photographed under an inverted microscope using a ×10 phase objective [29]. Cell areas were measured randomly (200 cells per fraction) using Scion Image

software (Scion Corp., Frederick, MD, http://www.scioncorp.com/) and statistically analyzed.

5-Bromo-2′-deoxyuridine Cell Proliferation Assay

The proliferative capacity of each isolated cell fraction was determined by 5-bromo-2′-deoxyuridine (BrdU) enzyme-linked immunosorbent assay (ELISA) cell proliferation assay (Amersham Biosciences, Freiburg, Germany, http://www.amersham.com) using a previously reported protocol [20, 30]. Analysis was on the 6th day of passage ($n = 3$). Cultured cells were incubated with 10 μM BrdU-labeling solution (20 hours, 37°C), washed with 250 μl of PBS containing 10% serum per well, fixed with 70% ethanol in hydrochloric acid (30 minutes, −20°C), and incubated with 100 μl of monoclonal antibody against BrdU (90 minutes), and then 100 μl of peroxidase substrate was added to each well. BrdU absorbance in each well was measured directly with a spectrophotometric microplate reader at a test wavelength of 450 nm and a reference wavelength of 490 nm. This measure of the degree of cell proliferation we termed the proliferation index. Each sample was cultured in triplicate.

The proliferative capacity of isolated p75(+) cells incubated with several neurotrophins (NGF, NT-3, NT-4, and BDNF) was also analyzed using the same procedure. The p75(+) cells were seeded at a density of 2×10^2 cells per cm^2 for 48 hours. Next, the cells were preincubated with the aforementioned neurotrophins (1, 10, and 100 ng/ml, respectively) for an additional 48 hours and then analyzed.

Colony-Forming Efficiency

The clonal growth ability of each isolated cell fraction was determined by colony-forming efficiency (CFE) assay. Cells (2×10^3) were plated on six-well culture dishes that contained a feeder layer of MMC-inactivated NIH-3T3 fibroblasts ($n = 3$). The colonies were fixed on day 7, stained with 0.1% truidine blue, and counted independently by three investigators; the data were then averaged. Each sample was cultured in triplicate. CFE was defined as the ratio of the number of colonies to the number of viable cells seeded.

Ex Vivo Expansion of Isolated Cells

To culture isolated cell fractions we used our previously reported system [18–20]. Isolated cells (1×10^5 cells per well) were then seeded onto denuded amniotic membrane (AM) spread on the bottom of culture inserts, and cocultured for 10 days with mitomycin C-inactivated 3T3 fibroblasts (2×10^4 cells per cm^2). The culture medium consisted of a defined keratinocyte growth medium (ArBlast, Kobe, Japan, http://www.arblast.jp) supplemented with 5% fetal bovine serum. The percentage of Ki67(+) cells in the basal layer of cultivated epithelium was determined on tissue sections. We analyzed five different fields from samples obtained from three different donors (15 areas per donor).

Immunohistochemistry

Immunohistochemical studies followed our previously described method [18, 20]. Briefly stated, 3-μm-thick cryostat sections were placed on gelatin-coated slides, air-dried, and rehydrated in PBS at room temperature for 15 minutes. To block nonspecific binding, the tissues were incubated with 2% bovine serum albumin (room temperature, 30 minutes). The sections were then incubated (room temperature, 1 hour) with the appropriate primary antibody (simple antibody or a mixture of antibodies for double staining) and washed (three times) in PBS containing 0.15% Triton X-100 for 15 minutes. Control incubations were with the appropriate normal mouse and rabbit IgG (Dako) at the same concentration as the primary antibody; the primary antibody for the respective specimen was omitted. After staining with the primary antibody, the sections were incubated with the appropriate secondary antibodies (room temperature, 1 hour), washed several times with PBS, coverslipped using antifading mounting medium containing propidium iodide or 4,6-diamidino-2-phenylindole (Vectashield; Vector Laboratories, Burlingame, CA, http://www.vectorlabs.com), and examined under a confocal microscope (Olympus Fluoview).

Real-Time PCR

Quantitative real-time PCR for p75, integrin β1, integrin α6, CD71, and ABCG2 was performed using an ABI Prism 7000 instrument (Applied Biosystems, Foster City, CA, http://www.appliedbiosystems.com). Total RNA was isolated with the RNeasy Micro Kit (Qiagen, Tokyo, http://www1.qiagen.com) ($n = 5$). We then performed quantitative real-time reverse transcription (RT)-PCR using QuantiTect Probe RT-PCR kits (Qiagen). Primers and probes for p75, integrin β1, integrin α6, CD71, ABCG2, and β-actin were from Applied Biosystems. For relative quantification, we used the ΔC_T method (Applied Biosystems). Analyses were performed in a sequence detector (ABI Prism 7000) using the accompanying data analysis software.

Apoptosis Assay

The p75(+) cells were seeded at a density of 2×10^2 cells per cm^2 on a chamber slide for 48 hours. Next, the cells were preincubated with several neurotrophins (100 ng/ml) for 48 hours, with or without UV irradiation (25 mJ per cm^2) [31]. The cells were directly stained by the In Situ Apoptosis Detection Kit (terminal deoxynucleotidyl transferase dUTP nick-end labeling [TUNEL] assay; Takara).

RESULTS

In Vivo Expression Patterns and Cell-Cycling Status of p75(+) Human Oral Keratinocytes

The in vivo expression patterns of p75 in human oral mucosal epithelium were investigated by indirect immunofluorescence. We used p75 antibodies from three companies (Chemicon, Abcam, and Upstate Biotech) and found no differences in the immunohistochemical results. We obtained tissues from the buccal mucosa (representing lining mucosa), where rete ridges are comparatively shallow and gentle, and gingiva (representing masticatory mucosa), where they are steep and deep. In the buccal mucosa, we noted intensive p75 expression primarily in the basal cell layer of the tips of the papillae (Fig. 1A); in some parts, p75 was expressed in deep rete ridges (Fig. 1B). In the gingiva, it was exclusively expressed in the basal cell layer of both the tips of the papillae and the deep rete ridges (Fig. 1C). In both tissues, p75 was expressed in the cell membrane. The immunostaining patterns suggest cluster (patch) organization, and clusters of brightly fluorescent basal cells were interspersed with stretches of basal cells with little or no fluorescence. The percentage of p75(+) cells per total oral keratinocytes was 7.35 ± 3.41 (five different fields from six different donors [total, 30 sections] were analyzed).

Slow or infrequent cycling is one of the unique features of adult SCs [32–37]. To investigate the in vivo cell cycle status in human oral mucosal epithelium, we used double immunostaining with p75 and Ki67, a marker for actively cycling cells. Ki67 was primarily expressed in the suprabasal and occasionally in the basal cell layer of oral epithelium (Fig. 1D, 1E). Statistical analysis of our double-staining results on 32 sections (5–10 sections each from four different donors) showed that among the p75(+) cells, the proportion of Ki67(−) cells was significantly higher (96.63% ± 2.69%) than that of Ki67(+) cells (3.37% ± 2.68%) (*, $p < .001$, t test), indicating that in vivo, most p75(+) cells were not actively cycling cells (Fig. 1F).

Characteristics of p75(+) and p75(−) Cell Fractions

To examine the characteristics of the p75(+) and p75(−) cell fractions, we isolated the subsets by magnetic cell sorting and validated our results by flow cytometry, RT-PCR, and immunofluorescence (supplemental online Fig. 1). Flow cytometric analysis showed that our use of a combination of depletion and positive selection columns yielded a purity in excess of 92% for

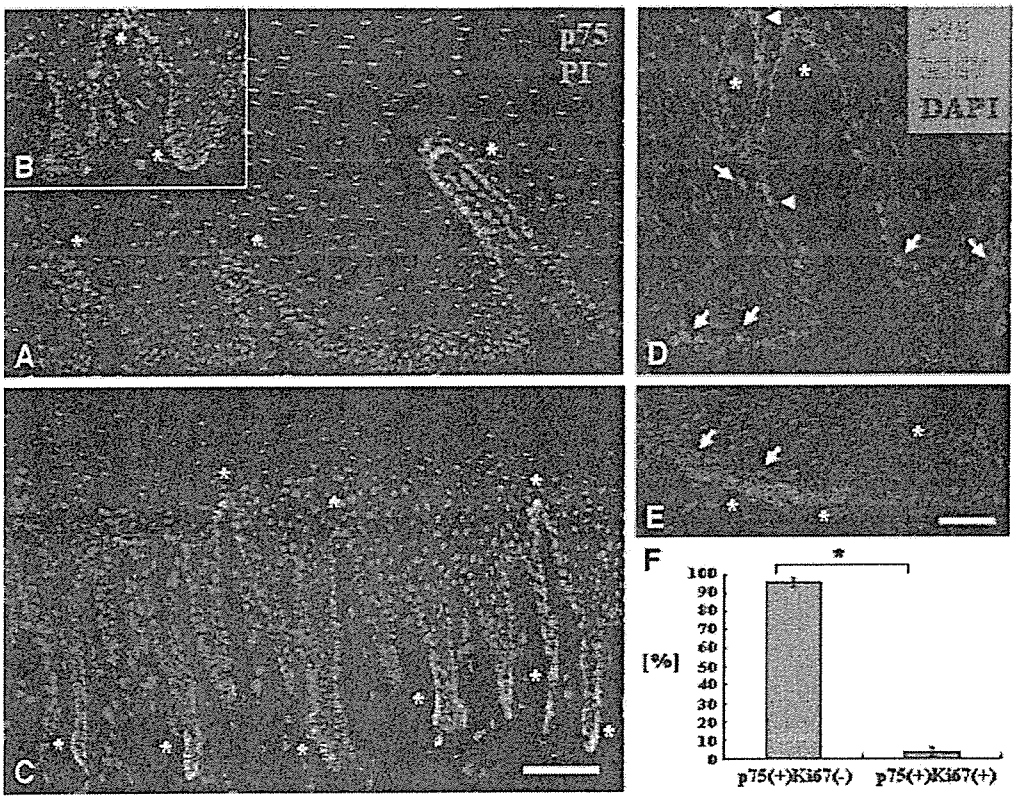

Figure 1. Immunolocalization of p75 and p75-Ki67 in human oral mucosal tissues. **(A–C):** In buccal mucosa, rete ridges are relatively shallow and gentle: p75 expression was intense primarily in the basal cell membrane of the tips of the papillae **(A)** (*). There was p75 expression in some deep rete ridges **(B)** (*). In the gingiva, rete ridges are deep and steep; p75 was expressed exclusively in the basal cell layer of the tips of the papillae and the deep rete ridges **(C)** (*). Patches of brightly fluorescent basal cells were interspersed with stretches of basal cells showing no or little fluorescence. **(D–F):** Ki67 expression was mainly observed in the suprabasal cell layer and occasionally in the basal cell layer of oral epithelium **(D, E)**. The percentages of Ki67(−) and Ki67(+) cells among all p75(+) cells were 96.63% ± 2.69% and 3.37% ± 2.68%, respectively **(F)**. The difference was statistically significant (*, $p < .001$, t test). Asterisks and arrows indicate clusters of p75(+) and Ki67(+) cells, respectively. Arrowheads indicate p75(+) Ki67(+) cells. Scale bars = 100 μm. Abbreviations: DAPI, 4,6-diamidino-2-phenylindole; PI, propidium iodide.

p75(+) cells in all experiments (supplemental online Fig. 1A). RT-PCR and immunofluorescence for p75 confirmed its expression at both the mRNA and protein level in the purified fraction (supplemental online Fig. 1B, 1C).

As the highest clonogenicity, a feature of SCs, is reportedly found in the smallest keratinocytes [29], we measured the cell size in each isolated fraction using Scion Image software. Under an inverted microscope, p75(+) cells were clearly smaller than p75(−) cells (Fig. 2A). The average size of p75(+) cells was significantly smaller than that of p75(−) cells (102.52 ± 46.85 vs. 346.84 ± 134.67 μm^2; *, $p < .001$, t test) (Fig. 2A).

The proliferative capacity and clonal growth ability of each isolated cell fraction was determined by BrdU ELISA cell proliferation assay and CFE. Phase-contrast inspection of the isolated cells on the 6th day of passage showed that p75(+) cells formed colonies consisting of ovoid and round cells (Fig. 2B); p75(−) cells, which did not form colonies, were large and elongated (Fig. 2B). The proliferation indexes of p75(+) and p75(−) cell fractions were significantly different (9.64 ± 0.1 vs. 1.16 ± 0.09; *, $p < .001$, t test) (Fig. 2B), as was the CFE (10.1% ± 1.2% vs. 0.19% ± 0.07%; *, $p < .001$, t test) (Fig. 2C), indicating that the p75(+) fraction manifested greater in vitro proliferative capacity than the p75(−) fraction.

To evaluate their in vitro tissue-forming ability, we cultivated isolated cell fractions on an AM substrate. After 10 days of cultivation, p75(+) oral epithelial cells formed 4–5 layers exhibiting well-conserved columnar basal cells and progressive flattening toward the surface (p75(+) sheet). On the other hand, p75(−) cells grew in monolayers composed of elongated, differentiated cells (Fig. 2D). To assess the cell-cycling status of these cultivated oral epithelial cells we examined their expression of Ki67. In p75(+) and p75(−) sheets, Ki67-labeled cells constituted 81.3% ± 10.6% and 25.4% ± 9.9%, respectively (Fig. 2D), rendering the difference in the Ki67-labeling index statistically significant (*, $p < .001$, t test).

Using immunofluorescence and specific markers, we studied the morphological and biological characteristics of the p75(+) and p75(−) sheets. ZO-1, a tight junction-related component, was expressed in the apical surface on p75(+) but not p75(−) sheets (Fig. 3A, 3B). Desmoplakin, a cell-cell junction component, was clearly expressed in the cell membrane on p75(+) sheets; there was moderate desmoplakin expression on p75(−) sheets (Fig. 3C, 3D). On p75(+) sheets, nonkeratinized, mucosa-specific keratin 4 was expressed in the superficial layer and the upper half of the intermediate layer; keratin 13 was expressed in all but the basal cell layers (Fig. 3E, 3G). On p75(−) sheets, on the other hand, there was no or faint superficial staining (Fig. 3F, 3H). The basement membrane assembly proteins integrin $\alpha 6/\beta 4$ showed linear positive staining on the basement membrane side on both p75(+) and p75(−) sheets (Fig. 3I–3L). Integrin $\alpha 3$ was mainly expressed in the basal cell membrane on both p75(+) and p75(−) sheets (Fig. 3M, 3N), and

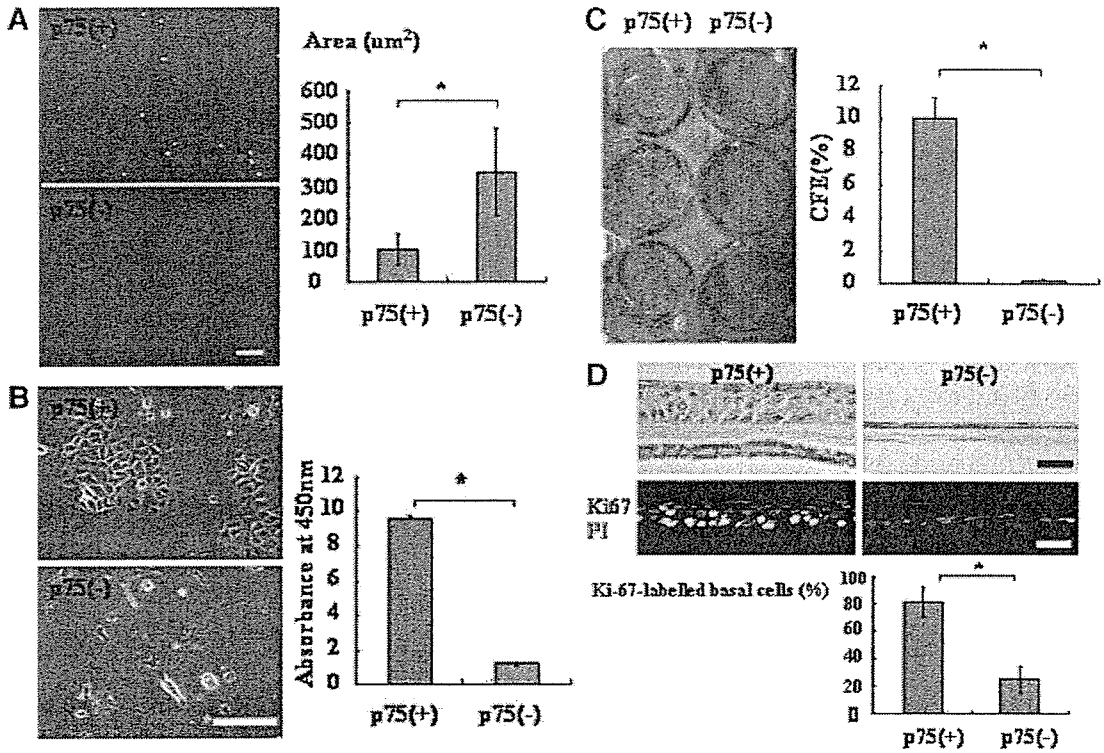

Figure 2. Characteristics of p75(+) and p75(−) cell fractions. **(A):** Under an inverted microscope, p75(+) cells are clearly smaller than p75(−) cells. The average cell size of the p75(+) cell fraction was 102.52 ± 46.85 μm^2, significantly smaller than the 346.84 ± 134.67 μm^2 of the p75(−) cell fraction (*, $p < .001$, t test). Scale bars = 100 μm. **(B):** Phase-contrast of isolated cells on the 6th day of passage. p75(+) cells formed colonies with ovoid and round cells; p75(−) cells did not form colonies and presented as large elongated cells. 5-Bromo-2′-deoxyuridine enzyme-linked immunosorbent assay showed that the proliferation indexes of p75(+) and p75(−) cell fractions was 9.64 ± 0.1 and 1.16 ± 0.09, respectively. The difference was statistically significant (*, $p < .001$, t test). **(C):** The clonal growth ability of isolated cell fractions was determined by CFE assay. Cells (2×10^3) were plated on six-well culture dishes containing a feeder layer of mitomycin C-inactivated NIH-3T3 fibroblasts. Colonies were fixed on day 7 and stained with 0.1% truidine blue. The CFEs of p75(+) and p75(−) cells were 10.1% ± 1.2% and 0.19% ± 0.07%, respectively, and the difference was statistically significant (*, $p < .001$, t test). **(D):** On the amniotic membrane (AM) substrate, p75(+) oral epithelial cells formed four to five layers. Note the well-conserved columnar basal cells and the progressive flattening toward the surface. Cultivated p75(−) cells grew in monolayers and consisted of elongated differentiated cells. Of the total basal cells in p75(+) and p75(−) sheets, 81.3% ± 10.6% and 25.4% ± 9.9%, respectively, were Ki67-labeled. The difference in the Ki67-labeling index in the isolated cell fractions was statistically significant (*, $p < .001$, t test). Scale bars = 100 μm. Abbreviations: CFE, colony-forming efficiency; PI, propidium iodide.

integrin β1 was expressed in the cell membrane of nearly all epithelial cells on p75(+) sheets; moderate or faint integrin β1 staining was observed on p75(−) sheets (Fig. 3O, 3P). Thus, only the p75(+) sheets manifested normal cell differentiation and normal junctional specialization, suggesting that only the p75(+) cells possessed high in vitro proliferative capacities and normal three-dimensional (3D) tissue formation potential.

Isolation and Clonal Analysis of Oral Keratinocyte SCs

To determine whether holoclones, meroclones, and paraclones, previously identified in human epithelium [9–11, 38], are also present in human oral mucosal epithelium, we isolated single cells from eight different primary cultures obtained from eight different donors (four buccal mucosa, four gingiva). We analyzed 396 clones; of these, 56.9% ± 22.8% formed original clones (Table 1). Photographs of representative holoclones, meroclones, and paraclones are shown in Figure 4. According to Barrandon and Green [9] and Pellegrini et al. [11], the representative original clone of the holoclone is large, has a smooth perimeter, and contains mainly small cells (Fig. 4A); most original clones of the paraclone are small and contain large differentiated squamous cells (Fig. 4C), and the meroclone is intermediate between the holoclone and the paraclone (Fig. 4B). On indicator dishes, holoclones formed large, rapidly growing colonies, fewer than 5% of which aborted or terminally differentiated (Fig. 4D). The paraclone grew no colonies or only uniformly small, terminal colonies (Fig. 4F), and the meroclone formed growing and aborted colonies (Fig. 4E). Of the clones studied, 23.6% ± 12.5% were holoclones, 34.9% ± 10.5% were meroclones, and 41.5% ± 11.3% were paraclones (Table 1). Our findings indicate that holoclone-, meroclone-, and paraclone-type cells, previously identified in skin and ocular surface, also comprise the proliferative compartment of the human oral mucosal epithelium.

To investigate the expression of p75 and integrin β1 in these three clonal types, we performed immunohistochemical analysis and real-time PCR assay. Immunofluorescence showed that p75 was strongly expressed in the membrane of holoclone cells (Fig. 4G), moderately expressed in some of the small cells of meroclones (Fig. 4H), and not expressed in paraclone cells (Fig. 4I). In contrast, integrin β1 was expressed in all three clonal types (Fig. 4J–4L). We used real-time PCR to assess p75 mRNA expression (supplemental online Fig. 2) and found that compared with meroclone and paraclone cells, in holoclone cells, mean p75 mRNA expression was significantly upregulated (*, $p < .05$, Mann-Whitney U test); all three clonal type cells

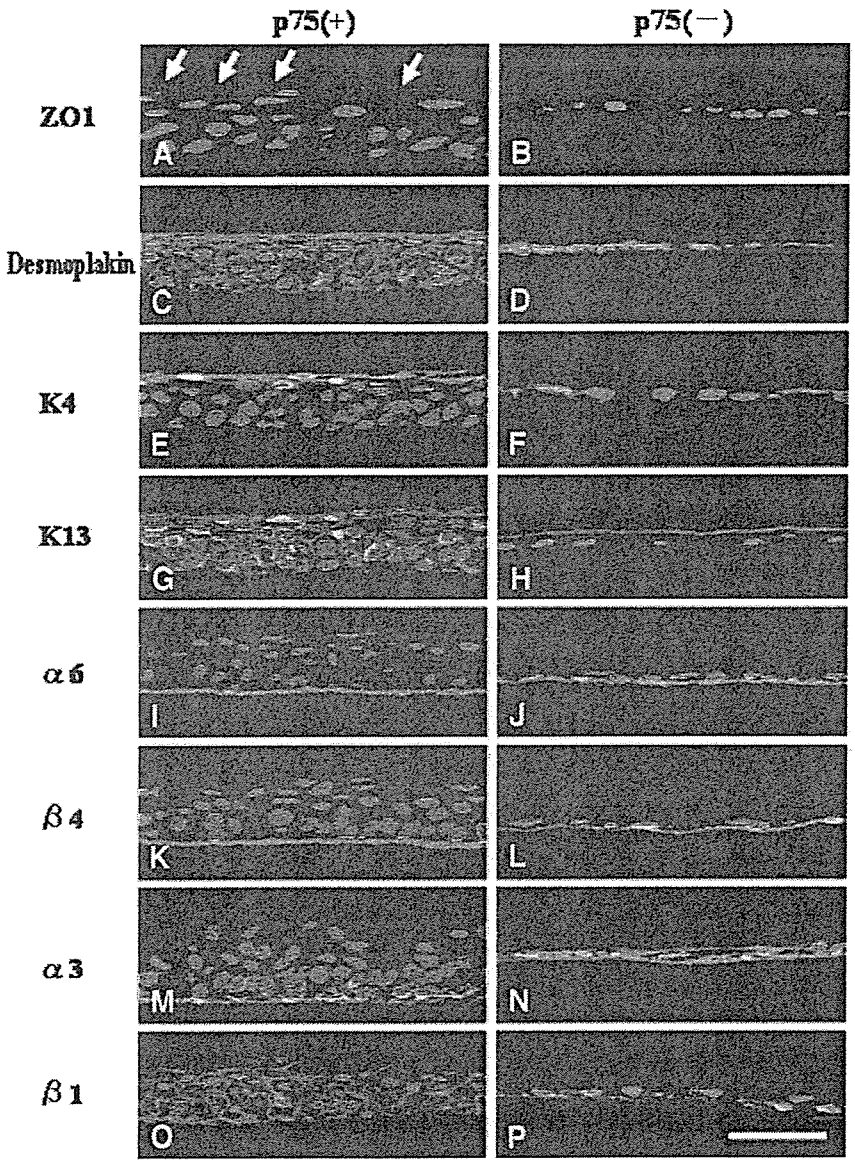

Figure 3. Representative immunofluorescence micrographs of p75(+) and p75(−) oral epithelial cells grown on amniotic membrane. ZO-1 was expressed on the apical surface of the p75(+) sheet but not the p75(−) sheet (**A, B**). Desmoplakin was clearly expressed in the cell membrane of the p75(+) sheet and moderately expressed in the p75(−) sheet (**C, D**). In the p75(+) sheet, mucosal-specific keratin 4 was expressed in the superficial portion and the upper half of the intermediate layers; keratin 13 was expressed in all epithelial layers except the basal cell layers (**E,G**). In the 75(−) sheet, there was no or faint superficial staining (**F, H**). The basement membrane assembly proteins integrin $\alpha 6/\beta 4$ showed linear positive staining on the basement membrane side of both p75(+) and p75(−) sheets (**I–L**). In both p75(+) and p75(−) sheets, integrin $\alpha 3$ was mainly expressed in the basal cell membrane (M, N). Integrin $\beta 1$ was expressed in the cell membrane of nearly all epithelial cells in the p75(+) sheet; only faint or moderate staining was observed in the p75(−) sheet (**O, P**). Scale bars = 100 μm.

exhibited integrin $\beta 1$ mRNA expression. These findings showed that p75 was strongly expressed in holoclone-type cells, suggesting p75 as a potential marker for oral keratinocyte SC-containing populations.

The Role of Neurotrophin Signaling in p75(+) Oral Keratinocytes

To evaluate the role of neurotrophin/p75 signaling in cell growth, differentiation, and survival, we performed the BrdU ELISA cell proliferation assay, immunohistochemistry for differentiation markers (keratin 10 and 13), and UV-induced apoptosis assay (TUNEL) in the presence or absence of neurotrophins in an in vitro culture system. BrdU assay indicated that NGF and NT-3 stimulated p75(+) oral keratinocyte cell proliferation (Fig. 5; *, $p < .01$, t test). From our immunohistochemical results, there were no differences regarding the effect of neurotrophins on cell differentiation. All p75(+) cells incubated with neurotrophins showed the expression of mucosal-specific keratin 13 but not keratinization-specific keratin 10 (supplemental online Fig. 3). TUNEL assay indicated that neurotrophins other than NGF fail to protect p75(+) oral keratinocytes from UV-induced apoptosis (Fig. 6). Our in vitro findings indicate that some neurotrophin/p75 signaling affects cell growth and survival but not cell differentiation.

Discussion

The role of SCs in homeostasis, wound healing, and tumorigenesis and their identification and therapeutic use in tissue engineering, gene therapy, and the treatment of various diseases have gained attention. In view of ethical concerns surrounding the use of embryonic SCs, the identification of specific markers to isolate keratinocyte SC populations is of great value, both for a better understanding of SCs and for the development of SC-mediated regenerative therapies. We demonstrated the following points: (a) that p75(+) cell subsets are present as clusters in a specific region of the human oral mucosal epithelium and (b) that most of these cells do not cycle actively in vivo. Cell sorting showed that compared with p75(−) cells, p75(+) cells

Table 1. Classification of clonal types

Donor age/gender	Tissue origin	Original clone formation (%)	Each type of clone (%)		
			Holoclone	Meroclone	Paraclone
18/M	Buccal	16.7	16.7	33.3	50
29/F	Buccal	61	18.1	36.4	45.5
37/M	Buccal	75	16.7	50	33.3
44/M	Buccal	50	22.3	22.7	50
19/F	Gingiva	80.6	34.5	24.1	41.4
24/F	Gingiva	75	50	27.8	22.2
25/M	Gingiva	30.6	13.6	34.5	56.4
27/F	Gingiva	66.7	16.7	50	33.3
		56.9 ± 22.8	23.6 ± 12.5	34.9 ± 10.5	41.5 ± 11.3

Abbreviations: F, female; M, male.

(c) were smaller and (d) had higher in vitro proliferative capacity and clonal growth potential. Our single-cell clonal analysis revealed (e) that three clonal types, previously identified in skin and ocular surface, also comprise the proliferative compartment of human oral mucosal epithelium and (f) that p75 is strongly expressed in holoclones at both the mRNA and protein level. Our in vivo and in vitro findings indicate that p75 may represent a novel marker for oral keratinocyte SC-containing populations.

In this study, we demonstrate for the first time that human oral keratinocytes exhibit regional diversity with respect to p75 expression. In the buccal mucosa, p75 was mainly expressed in the tips of the papillae, whereas in gingiva it was observed in both the tips of the papillae and the deep rete ridges. In the current situation, we can not exactly determine whether this means there are two stem cell niches in gingiva. The precise location of stem/progenitor cells within the epithelium is a question that remains to be settled, and its proposed answer depends on the expression pattern, cell surface markers, specific tissues, and species. Others [12, 13] reported that SC distribution is nonrandom but varies by the specific phenotype of epithelial tissue. They found that cells brightly stained for integrin β1, a putative epidermal SC marker, were located in the tips of dermal papillae in human foreskin and interfollicular scalp and in the deep rete ridges of the palm.

These cells, as was the case in our p75(+) cells, existed as clusters in tissue, rather than as sporadic single cells. Lavker and Sun [4, 7] studied the morphological and functional characteristics of epidermal SC located at different sites. Keratinocytes at the bottom of the rete ridges in foreskin and interfollicular scalp are protected, pigmented, and ultrastructurally primitive. They express less integrin β1 than basal cells in the shallowest portion (tips of the papillae) of these areas of the epidermis. However, the latter tend to be more specialized ultrastructurally and are more vulnerable to environmental insults than basal cells located in the deep rete ridges. Our in vivo and in vitro findings indicate that p75 is a potential marker of oral keratinocytes in both stem and progenitor cells, so regarding the p75 expression pattern, we do not consider that there are two stem cell niches, but rather either the deep or shallow portion of the rete ridges are stem cell-containing compartments. We posit that from the recent reports using a cell surface marker for Dsg3 [39] and K15 [40], the location of stem and transient amplifying cells tends to be in the tips of the deep rete ridges. Additional cell biological studies are needed to clarify this point.

It is important to clarify how high p75 expression can better define human oral keratinocyte stem/progenitor cells compared with other previously reported epidermal keratinocyte SC phenotypes, such as integrin β1 [12, 41], integrin α6/CD71 [14, 15], and side population (SP) cells [42–45]. We also investigated the expression of CD34, a mouse bulge cell marker, and found that like previous reports on human bulge cells [46–48], it was not expressed in any layer of human oral mucosal epithelium (data not shown). To elucidate the relationship between p75 and integrin β1, integrin α6/CD71, and SP, we investigated their expression level in all isolated p75(+) and p75(−) cell fractions using real-time PCR (supplemental online Fig. 4). Moreover, we have investigated the expression of these proposed epidermal SC markers and compared them with the expression of p75 in the serial cross sections using the appropriate mouse monoclonal antibodies (supplemental online Fig. 5). Real-time PCR showed that the level of integrin β1 and ABCG2 mRNA in the p75(+) cell fraction was higher than that of the p75(−) cell fraction (supplemental online Fig. 4A, 4B; *, $p < .01$). Although there was some tendency toward a decreased CD71 mRNA level in p75(+) cell fractions, the level of both integrin α6 and CD71 mRNA was not statistically significant (supplemental online Fig. 4C, 4D). Immunohistochemical analysis showed that integrin β1 was expressed in their basal and suprabasal cell layers (supplemental online Fig. 5B). The expression of p75 was observed in the restricted region of the basal cell layer (supplemental online Fig. 5A, 5C, 5F, *). Interestingly, immunohistochemistry showed that CD 71 was mainly expressed in the basal and suprabasal cells of human oral mucosal epithelium, and negative or low levels of CD71 cells were sporadically observed in the deep rete ridges (supplemental online Fig. 5D, *). Furthermore, BCRP1 was observed in the restricted region of the basal cells of human oral mucosal epithelium (supplemental online Fig. 5G, *). Based on these findings, the expression pattern of the proposed epidermal SC markers was partially overlapped but somewhat different from that of p75, suggesting that p75(+) oral keratinocytes may have different features from the proposed epidermal SC markers. However, these results alone do not allow us to fully explain the differences between p75 and proposed epidermal keratinocyte SC markers, and additional studies are under way in our laboratory to determine the precise character of p75(+) human oral keratinocytes.

Under steady-state conditions, SCs divide infrequently in vivo [49, 50]. However, they can proliferate vigorously in vitro and after appropriate stimulation in vivo. TACs, on the other hand, cycle actively. Cell kinetic studies, such as the label-retaining method, are clearly considered the gold standard by which to identify slow-cycling SCs. However, it is difficult to perform these kinds of cell kinetic studies in humans due to ethical considerations. Therefore, it is necessary to establish a useful assay to assign SC status isolated on the basis of biological markers in humans. In our study, most p75(+) basal cells did not express the proliferation-associated marker Ki67, suggesting that they did not cycle actively in vivo. Our finding that the human oral mucosal epithelium contained a small subset of p75(+)-Ki67(+) cells suggests that p75, although valuable for

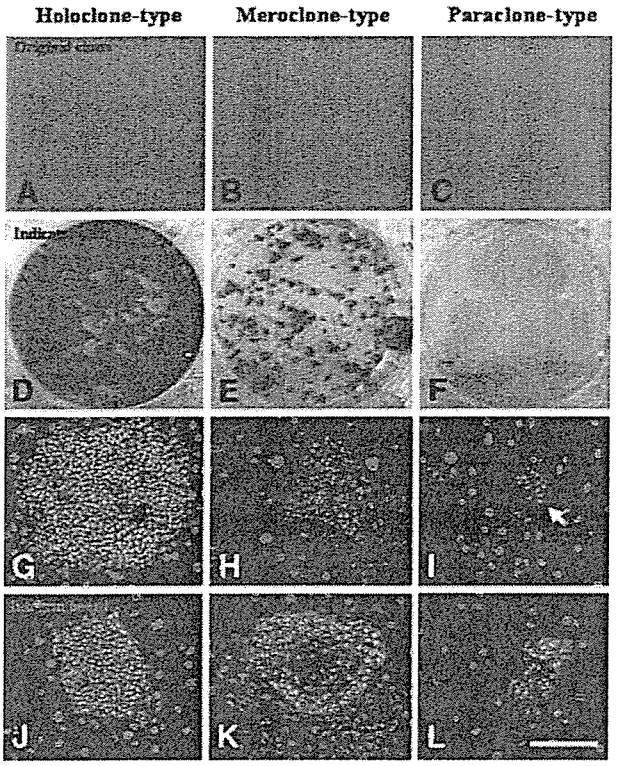

Figure 4. Isolation and clonal analysis of oral keratinocytes. The representative original clone of the holoclone type is large, has a relatively smooth perimeter, and contains mainly small cells (**A**). Most original clones of the paraclone type are small and contain large differentiated squamous cells (**C**). The meroclone type is intermediate between the holoclone and the paraclone (**B**). Toluidine blue staining (indicator dishes) clearly showed that the holoclone formed large, rapidly growing colonies, fewer than 5% of which aborted or differentiated terminally (**D**). The paraclone grew no colonies or only uniformly small terminal colonies (**F**). The meroclone formed growing and aborted colonies (**E**). Immunofluorescence showed that p75 was strongly expressed in the cell membrane of holoclone-type cells (**G**). In the meroclone-type cells, p75 was moderately expressed in some of the small cells (**H**). Paraclone-type cells did not express p75 (**I**). In contrast, integrin $\beta 1$ was expressed in the cell membrane of all three clonal types (**J–L**). Scale bars = 100 μm.

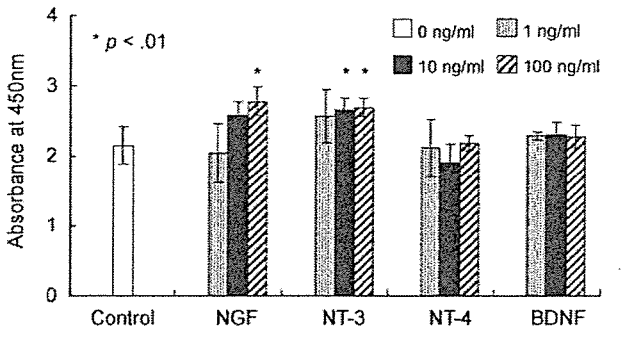

Figure 5. Neurotrophin effects on oral keratinocyte proliferation. 5-Bromo-2′-deoxyuridine (BrdU) enzyme-linked immunosorbent assay cell proliferation assay of p75 (+) oral epithelial cells cultivated in the presence (1, 10, and 100 ng/ml) and absence of neurotrophin (NGF, NT-3, NT-4, and BDNF)-supplemented media for 48 hours (n = 5). Scale bars indicate the mean values of BrdU absorbance in each culture condition. BrdU assay indicated that NGF and NT-3 stimulated p75(+) oral keratinocyte cell proliferation (*, $p < .01$, t test). Abbreviations: BDNF, brain-derived neurotrophic factor; NGF, nerve growth factor; NT, neurotrophin.

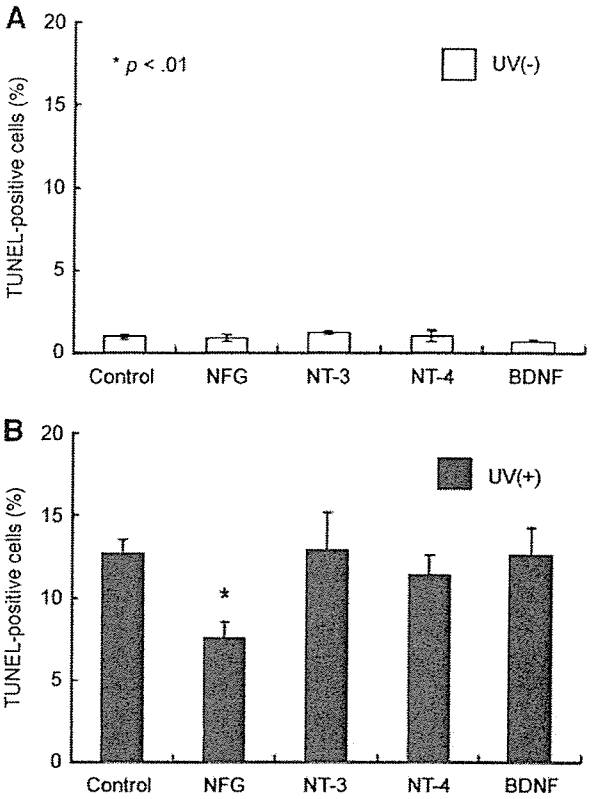

Figure 6. Neurotrophin effects on oral keratinocyte cell survival. The p75(+) oral epithelial cells were treated for 48 hours in the presence (100 ng/ml) and absence of neurotrophin (NGF, NT-3, NT-4, and BDNF)-supplemented media before, with, or without UV irradiation, and apoptosis was measured by TUNEL staining. The percentage of TUNEL(+) cells in each culture condition was calculated by three individual experiments. Without UV conditions, neurotrophins do not seem to influence cell death in these cells (**A**). Under UV(+) conditions, NGF exerts a protective effect against UV-induced apoptosis (*, $p < .01$, t test); however, the other neurotrophins do not prevent cell death (**B**). Abbreviations: BDNF, brain-derived neurotrophic factor; NGF, nerve growth factor; NT, neurotrophin; TUNEL, terminal deoxynucleotidyl transferase dUTP nick-end labeling.

sorting SC populations, may also identify early TAC populations on the basis of their cell-cycling status.

Others reported that cell size may distinguish SCs from TACs or differentiated cells. In the epidermis, the response to phorbol esters of the smallest keratinocytes is different from that of other cells [51, 52]. These keratinocytes also exhibited the highest clonogenicity; cultured keratinocytes isolated from human epidermis formed clones when they were 11 μm or less in diameter, and they terminally differentiated when they were 12 μm or more in diameter [29]. The average diameter of our p75(+) cells was 11.4 ± 3.8 μm, which is consistent with the report of Barrandon and Green [29]. Based on these findings and on the reported size of corneal epithelial SCs [53], we suggest that cell size is a potential indicator of keratinocyte SCs, not only of the epidermis, but also of other epithelial cell types.

We found that isolated keratinocytes fractionated on the basis of the intensity of their p75 expression could produce different cell populations with different properties. Only cells in the p75(+) population exhibited exceptionally high proliferative potential, CFE, and 3D tissue forming-ability, features associated with SC populations and consistent with esophageal keratinocyte SCs studied in vitro [28]. However, SC-rich fractions from adult rat epidermis [54] and neonatal human foreskin [55]

manifested substantially lower CFE than the source populations. Moreover, in standard tissue cultures, exhaustion of the proliferative potential of keratinocytes can be slowed by amending the culture conditions [56]. These discrepancies may be related to species differences (human and rodent), the cell isolation techniques used, and the biological state of the keratinocyte SCs in culture. Although the cell-sorting procedure using specific cell-surface markers is useful [12, 55], the isolated cells are released from the control mechanisms regulating the in vivo SC niche that renders them slow-cycling.

Although cultured human keratinocytes may not retain all their in vivo characteristics after removal from their microenvironment, they are clonogeneic [12, 13, 49] and able to generate three distinct clonal forms due to the varied self-renewal capacities of individual keratinocytes [9]. Analysis of clonal-type frequency after a period of in vitro growth yields information on the intrinsic nature and proliferative potential of the original keratinocyte populations. The three clonal types we identified (holoclone, meroclone, and paraclone) comprise the proliferative compartment of the human oral mucosal epithelium. As p75 was intensively expressed only by holoclone cells on both the mRNA and protein level, it may specifically characterize human oral keratinocyte SC-containing population.

In contrast, integrin $\beta 1$, an epidermal SC marker, was expressed in all three clonal-type cells. According to De Luca et al. [57] and Nguyen et al. [58], keratinocyte SCs completely disappeared in most mitogenic tissue culture environments and exhibited marked changes in their expression of integrin and other markers. Cell-surface receptor molecules are particularly useful for isolating SC compartments; however, reliance on cell adhesion molecules alone may be inadequate for SC isolation because almost all basal keratinocytes express these molecules, which are essential for biological processes, to various degrees [14, 59–61]. Therefore, markers specific for in vivo keratinocyte SCs may differ from those of keratinocyte colonies grown in vitro.

We also posit that it is very important to carefully interpret the results of stem cell research. Our conclusion that p75 may represent a marker for a human oral keratinocyte stem cell-containing population was mainly based on the results obtained by short-term in vitro clonogenic assay and tissue-regenerative ability, not by in vivo long-term reconstitution assay [62–64]. We truly recognize that sustained epithelial tissue regeneration in an appropriate in vivo transplant model is likely to be the best functional definition of keratinocyte stem cells. Even though in vitro assay with development of culture techniques for keratinocytes is believed to reflect the extensive capacity expected of keratinocyte stem cells in vivo, at present our in vitro assay alone does not allow us to fully characterize the human oral keratinocyte stem cells. Even though it is quite difficult to transplant human oral keratinocytes onto the oral cavity site, both technically and methodologically, an additional in vivo long-term assay is needed to clarify these points.

In several cell types, the protein family of mammalian neurotrophins (NGF, BDNF, and NT-3/4/5) supports cell survival, differentiation, and plasticity [65, 66]. The elucidation of the role of neurotrophin/p75 signaling in oral keratinocyte stem cells is important for better understanding the mechanism of stem cell behavior. In our series, one of the representative neurotrophin molecules, "NGF," can support keratinocyte cell proliferation and protect the cells from apoptosis. These results were consistent with the previous reports using other cell types [31, 66–72]. We also pointed out that effects of neurotrophins are mediated via the activation of two different classes of plasma membrane receptor, high-affinity Trk tyrosine kinase receptors (TrkA, TrkB, and TrkC) and low-affinity p75 neurotrophin receptors that form complexes. For example, p75 modulates cell death in different models [73–75]. Proapoptotic signaling occurs when p75 is expressed alone without the coexpression of Trk receptors [76, 77]. Thus, the cell death-inducing or cell-survival actions of neurotrophins are strongly dependent on the relative expression of p75 and Trk receptors on the target-cell populations. Studies are under way to elucidate the relationship between p75 and Trk receptors in keratinocytes from human oral mucosal tissue.

We believe that one way to characterize distinct cell populations is to generate global gene expression profiles. Recently, several microarray profiles of mouse [37, 78] and human [46] hair follicle bulge cells were reported. In these results, upregulation of p75 has not been identified in the bulge cells, yet we consider that oral mucosal epithelium is fundamentally different from bulge cells and epidermis, which may explain why upregulation of p75 was not detected. Moreover, the data represent the average characteristics of a cell population, rather than the properties of individual cells.

Our study showed that oral keratinocytes expressing the p75(+) phenotype exhibited properties suggesting that they are equivalent to the SC-containing population. The degree of SC sorting made possible by p75 will allow the further fractionation and analysis of SC populations, thereby facilitating the identification of a set of additional SC markers unique to the epithelium. Systematic evaluation using cell-sorting techniques and clonal analysis will facilitate the identification and purification of these cells and greatly contribute to our understanding of SC biology. In addition, greater knowledge regarding SCs will provide a foundation for the development of treatments for epithelium-related diseases.

ACKNOWLEDGMENTS

We thank Yann Barrandon for advising the clonal analysis system, Narisato Kanamura and Takashi Amemiya for performing the oral biopsies, Hideo Honjyo for providing AM, and Hisayo Sogabe and Tomoko Horikiri for assisting with the culture procedures. This study was supported in part by Grants-in-Aid for Scientific Research from the Japanese Ministry of Health, Labor and Welfare (H16-Saisei-007) and by the Japanese Ministry of Education, Culture, Sports, Science and Technology (Kobe Translational Research Cluster), a research grant from the Kyoto Foundation for the Promotion of Medical Science, and the Intramural Research Fund of Kyoto Prefectural University of Medicine.

DISCLOSURES

The authors indicate no potential conflicts of interest.

REFERENCES

1 Watt FM. Terminal differentiation of epidermal keratinocytes. Curr Opin Cell Biol 1989;1:1107–1115.
2 Lajtha LG. Stem cell concepts. Differentiation 1979;14:23–34.
3 Leblond CP. The life history of cells in renewing systems. Am J Anat 1981;160:114–158.
4 Lavker RM, Sun TT. Heterogeneity in epidermal basal keratinocytes: Morphological and functional correlations. Science 1982;215:1239–1241.

5 Hall PA, Watt FM. Stem cells: The generation and maintenance of cellular diversity. Development 1989;106:619–633.
6 Potten CS, Loeffler M. Stem cells: Attributes, cycles, spirals, pitfalls and uncertainties. Lessons for and from the crypt. Development 1990;110: 1001–1020.
7 Lavker RM, Sun TT. Epidermal stem cells. J Invest Dermatol 1983;81: 121s–127s.
8 Reid LM. Stem cell-fed maturational lineages and gradients in signals: Relevance to differentiation of epithelia. Mol Biol Rep 1996;23:21–33.
9 Barrandon Y, Green H. Three clonal types of keratinocyte with different capacities for multiplication. Proc Natl Acad Sci U S A 1987;84:2302–2306.
10 Rochat A, Kobayashi K, Barrandon Y. Location of stem cells of human hair follicles by clonal analysis. Cell 1994;76:1063–1073.
11 Pellegrini G, Golisano O, Paterna P et al. Location and clonal analysis of stem cells and their differentiated progeny in the human ocular surface. J Cell Biol 1999;145:769–782.
12 Jones PH, Watt FM. Separation of human epidermal stem cells from transit amplifying cells on the basis of differences in integrin function and expression. Cell 1993;73:713–724.
13 Jones PH, Harper S, Watt FM. Stem cell patterning and fate in human epidermis. Cell 1995;80:83–93.
14 Tani H, Morris RJ, Kaur P. Enrichment for murine keratinocyte stem cells based on cell surface phenotype. Proc Natl Acad Sci U S A 2000;97:10960–10965.
15 Li A, Pouliot N, Redvers R et al. Extensive tissue-regenerative capacity of neonatal human keratinocyte stem cells and their progeny. J Clin Invest 2004;113:390–400.
16 De Luca M, Albanese E, Megna M et al. Evidence that human oral epithelium reconstituted in vitro and transplanted onto patients with defects in the oral mucosa retains properties of the original donor site. Transplantation 1990;50:454–459.
17 Hata K, Ueda M. Fabrication of cultured epithelium using oral mucosal cells and its clinical applications. Hum Cell 1996;9:91–96.
18 Nakamura T, Endo K, Cooper LJ et al. The successful culture and autologous transplantation of rabbit oral mucosal epithelial cells on amniotic membrane. Invest Ophthalmol Vis Sci 2003;44:106–116.
19 Nakamura T, Inatomi T, Sotozono C et al. Transplantation of cultivated autologous oral mucosal epithelial cells in patients with severe ocular surface disorders. Br J Ophthalmol 2004;88:1280–1284.
20 Nakamura T, Ang LP, Rigby H et al. The use of autologous serum in the development of corneal and oral epithelial equivalents in patients with Stevens Johnson syndrome. Invest Ophthalmol Vis Sci 2006;47:909–916.
21 Nishida K, Yamato M, Hayashida Y et al. Corneal reconstruction with tissue-engineered cell sheets composed of autologous oral mucosal epithelium. N Engl J Med 2004;351:1187–1196.
22 Pellegrini G. Changing the cell source in cell therapy? N Engl J Med 2004;351:1170–1172.
23 Inatomi T, Nakamura T, Koizumi N et al. The mid-term results of ocular surface reconstruction using cultivated autologous oral mucosal epithelial transplantation. Am J Ophthalmol 2006;141:267–275.
24 Rodriguez-Tebar A, Dechant G, Gotz R et al. Binding of neurotrophin-3 to its neuronal receptors and interactions with nerve growth factor and brain-derived neurotrophic factor. EMBO J 1992;11:917–922.
25 Smith CA, Farrah T, Goodwin RG. The TNF receptor superfamily of cellular and viral proteins: Activation, costimulation, and death. Cell 1994;76:959–962.
26 Dechant G, Barde YA. Signalling through the neurotrophin receptor p75NTR. Curr Opin Neurobiol 1997;7:413–418.
27 Botchkarev VA, Botchkareva NV, Albers KM et al. A role for p75 neurotrophin receptor in the control of apoptosis-driven hair follicle regression. FASEB J 2000;13:1931–1942.
28 Okumura T, Shimada Y, Imamura M et al. Neurotrophin receptor p75(NTR) characterizes human esophageal keratinocyte stem cells in vitro. Oncogene 2003;22:4017–4026.
29 Barrandon Y, Green H. Cell size as a determinant of the clone-forming ability of human keratinocytes. Proc Natl Acad Sci U S A 1985;82: 5390–5394.
30 Ang LP, Tan DT, Beuerman RW et al. Development of a conjunctival epithelial equivalent with improved proliferative properties using a multistep serum-free culture system. Invest Ophthalmol Vis Sci 2004;45: 1789–1795.
31 Marconi A, Vaschieri C, Zanoli S et al. Nerve growth factor protects human keratinocytes from ultraviolet-B-induced apoptosis. J Invest Dermatol 1999;113:920–927.
32 Bickenbach JR. Identification and behavior of label-retaining cells in oral mucosa and skin. J Dent Res 1981;60:1611–1620.
33 Cotsarelis G, Cheng SZ, Dong G et al. Existence of slow-cycling limbal epithelial basal cells that can be preferentially stimulated to proliferate: Implications on epithelial stem cells. Cell 1989;57:201–209.
34 Fortunel N, Batard P, Hatzfeld A et al. High proliferative potential-quiescent cells: A working model to study primitive quiescent hematopoietic cells. J Cell Sci 1998;111:1867–1875.
35 Lehrer MS, Sun TT, Lavker RM. Strategies of epithelial repair: Modulation of stem cell and transit amplifying cell proliferation. J Cell Sci 1998;111:2867–2875.
36 Braun KM, Niemann C, Jensen UB et al. Manipulation of stem cell proliferation and lineage commitment: Visualisation of label-retaining cells in whole mounts of mouse epidermis. Development 2003;130: 5241–5255.
37 Tumbar T, Guasch G, Greco V et al. Defining the epithelial stem cell niche in skin. Science 2004;303:359–363.
38 Mather MB, Ferrari G, Dellambra E et al. Clonal analysis of stably transduced human epidermal stem cells in culture. Proc Natl Acad Sci U S A 1996;93:10371–10376.
39 Wan H, Stone MG, Simpson C et al. Desmosomal proteins, including desmoglein 3, serve as novel negative markers for epidermal stem cell-containing population of keratinocytes. J Cell Sci 2003;116:4239–4248.
40 Webb A, Li A, Kaur P. Location and phenotype of human adult keratinocyte stem cells of the skin. Differentiation 2004;72:387–395.
41 Blanpain C, Lowry WE, Geoghegan A et al. Self-renewal, multipotency, and the existence of two cell populations within an epithelial stem cell niche. Cell 2004;118:635–648.
42 Terunuma A, Jackson KL, Kapoor V et al. Side population keratinocytes resembling bone marrow side population stem cells are distinct from label-retaining keratinocyte stem cells. J Invest Dermatol 2003;121: 1095–1103.
43 Triel C, Vestergaard ME, Bolund L et al. Side population cells in human and mouse epidermis lack stem cell characteristics. Exp Cell Res 2004; 295:79–90.
44 Yano S, Ito Y, Fujimoto M et al. Characterization and localization of side population cells in mouse skin. STEM CELLS 2005;23:834–841.
45 Redvers RP, Li A, Kaur P. Side population in adult murine epidermis exhibits phenotypic and functional characteristics of keratinocyte stem cells. Proc Natl Acad Sci U S A 2006;103:13168–13173.
46 Ohyama M, Terunuma A, Tock CL et al. Characterization and isolation of stem cell-enriched human hair follicle bulge cells. J Clin Invest 2006;116:249–260.
47 Cotsarelis G. Gene expression profiling gets to the root of human hair follicle stem cells. J Clin Invest 2006;116:19–22.
48 Cotsarelis G. Epithelial stem cells: A folliculocentric view. J Invest Dermatol 2006;126:1459–1468.
49 Potten CS, Morris RJ. Epithelial stem cells in vivo. J Cell Sci 1988;10: 45–62.
50 Cotsarelis G, Sun TT, Lavker RM. Label-retaining cells reside in the bulge area of pilosebaceous unit: Implications for follicular stem cells, hair cycle, and skin carcinogenesis. Cell 1990;61:1329–1337.
51 Furstenberger G, Gross M, Schweizer J et al. Isolation, characterization and in vitro cultivation of subfractions of neonatal mouse keratinocytes: Effects of phorbol esters. Carcinogenesis 1986;7:1745–1753.
52 Gross M, Furstenberger G, Marks F. Isolation, characterization, and in vitro cultivation of keratinocyte subfractions from adult NMRI mouse epidermis: Epidermal target cells for phorbol esters. Exp Cell Res 1987; 171:460–474.
53 Romano AC, Espana EM, Yoo SH et al. Different cell sizes in human limbal and central corneal basal epithelia measured by confocal microscopy and flow cytometry. Invest Ophthalmol Vis Sci 2003;44:5125–5129.
54 Pavlovitch JH, Rizk-Rabin M, Jaffray P et al. Characteristics of homogeneously small keratinocytes from newborn rat skin: Possible epidermal stem cells. Am J Physiol 1991;261:C964–C972.
55 Li A, Simmons PJ, Kaur P. Identification and isolation of candidate human keratinocyte stem cells based on cell surface phenotype. Proc Natl Acad Sci U S A 1998;95:3902–3907.
56 Rheinwald JG, Green H. Epidermal growth factor and the multiplication of cultured human epidermal keratinocytes. Nature 1977;265: 421–424.
57 De Luca M, Pellegrini G, Bondanza S et al. The control of polarized integrin topography and the organization of adhesion-related cytoskeleton in normal human keratinocytes depend upon number of passages in culture and ionic environment. Exp Cell Res 1992;202:142–150.
58 Nguyen BP, Ryan MC, Gil SG et al. Deposition of laminin 5 in epidermal wounds regulates integrin signaling and adhesion. Curr Opin Cell Biol 2000;12:554–562.
59 Peltonen J, Larjava H, Jaakkola S et al. Localization of integrin receptors for fibronectin, collagen, and laminin in human skin. Variable expression in basal and squamous cell carcinomas. J Clin Invest 1989;84:1916–1923.
60 Carter WG, Wayner EA, Bouchard TS et al. The role of integrins alpha 2 beta 1 and alpha 3 beta 1 in cell-cell and cell-substrate adhesion of human epidermal cells. J Cell Biol 1990;110:1387–1404.
61 Dowling J, Yu QC, Fuchs E. Beta4 integrin is required for hemidesmosome formation, cell adhesion and cell survival. J Cell Biol 1996;134:559–572.
62 Kolodka TM, Garlick JA, Taichman LB. Evidence for keratinocyte stem cells in vitro: Long term engraftment and persistence of transgene expression from retrovirus-transduced keratinocytes. Proc Natl Acad Sci U S A 1998;95:4356–4361.
63 Schneider TE, Barland C, Alex AM et al. Measuring stem cell frequency

in epidermis: A quantitative in vivo functional assay for long-term repopulating cells. Proc Natl Acad Sci U S A 2003;100:11412–11417.
64 Pouliot N, Redvers RP, Ellis S et al. Optimization of a transplant model to assess skin reconstitution from stem cell-enriched primary human keratinocyte populations. Exp Dermatol 2005;14:60–69.
65 Poo MM. Neurotrophins as synaptic modulators. Nat Rev Neurosci 2001;2:24–32.
66 Botchkarev VA, Yaar M, Peters EM et al. Neurotrophins in skin biology and pathology. J Invest Dermatol 2006;126:1719–1727.
67 Matsuda H, Coughlin MD, Bienenstock J et al. Nerve growth factor promotes human hemopoietic colony growth and differentiation. Proc Natl Acad Sci U S A 1988;85:6508–6512.
68 Kannan Y, Ushio H, Koyama H et al. 2.5S nerve growth factor enhances survival, phagocytosis, and superoxide production of murine neutrophils. Blood 1991;77:1320–1325.
69 Paus R, Luftl M, Czarnetzki BM. Nerve growth factor modulates keratinocyte proliferation in murine skin organ culture. Br J Dermatol 1994; 130:174–180.
70 Di Marco E, Mathor M, Bondanza S et al. Nerve growth factor binds to normal human keratinocytes through high and low affinity receptors and stimulates their growth by a novel autocrine loop. J Biol Chem 1993; 268:22838–22846.
71 Touhami A, Grueterich M, Tseng SC. The role of NGF signaling in human limbal epithelium expanded by amniotic membrane culture. Invest Ophthalmol Vis Sci 2002;43:987–994.
72 Marconi A, Terracina M, Fila C et al. Expression and function of neurotrophins and their receptors in cultured human keratinocytes. J Invest Dermatol 2003;121:1515–1521.
73 Carter BD, Kaltschmidt C, Kaltschmidt B et al. Selective activation of NF-kappa B by nerve growth factor through the neurotrophin receptor p75. Science 1996;272:542–545.
74 Frade JM, Rodriguez-Tebar A, Barde YA. Induction of cell death by endogenous nerve growth factor through its p75 receptor. Nature 1996; 383:166–168.
75 Yaar M, Zhai S, Pilch PF et al. Binding of beta-amyloid to the p75 neurotrophin receptor induces apoptosis. A possible mechanism for Alzheimer's disease. J Clin Invest 1997;100:2333–2340.
76 Carter BD, Lewin GR. Neurotrophins live or let die: Does p75NTR decide? Neuron 1997;18:187–190.
77 Yoon SO, Casaccia-Bonnefil P, Carter B et al. Competitive signaling between TrkA and p75 nerve growth factor receptors determines cell survival. J Neurosci 1998;18:3273–3281.
78 Morris RJ, Liu Y, Marles L et al. Capturing and profiling adult hair follicle stem cells. Nat Biotechnol 2004;22:411–417.

See www.StemCells.com for supplemental material available online.